TRANSIENT RESPONSE OF DAM-LIKE STRUCTURE SUBJECTED TO EARTHQUAKE

A thesis submitted in partial fulfilment of
the requirements for the degree of

MASTER OF TECHNOLOGY

IN

CIVIL ENGINEERING

by

SUSANTA BASU

DEPARTMENT OF CIVIL ENGINEERING
INDIAN INSTITUTE OF TECHNOLOGY
KANPUR

August, 1969

CERTIFICATE

Certified that this work on 'Transient Response of Dam-Like Structure Subjected to Earthquake' has been carried out under my supervision and that this has not been submitted elsewhere for a degree.

A V Setlur

(A.V. Setlur)
Department of Civil Engineering
Indian Institute of Technology
Kanpur

ACKNOWLEDGEMENT

The author expresses his deep sense of gratitude and indebtness to Dr. A.V. Setlur for his invaluable guidance and constant encouragement throughout this work.

His thanks are also due to Dr. Y.C. Das and Dr. A.H. Shah for their active interest and lively discussion on the problem. The author is also grateful to Dr. J.L. Sridhar Rao for providing useful references on this work.

The author feels it his pleasant duty to acknowledge help and cooperation of the staff of the Computer Centre of the Indian Institute of Technology, Kanpur, during the course of work. Finally, he wishes to express thanks to Mr. Kishore for the trouble he has taken in typing out the manuscript.

LIST OF CONTENTS

LIST OF ILLUSTRATIONS

NOTATIONS

1. General Symbols

A^c : Cross-sectional area

A_o^c : Cross-sectional area at base

$\bar{A}$: Nondimensional area = A^c/A_o^c

A^w : Area of water moving with the dam

$\bar{a}$: Nondimensional angular velocity = $\psi_t L/k_1$

b : Width of water

C : Fundamental critical damping = $2 \rho^c A^c \omega_f$

$\bar{C}$: Damping constant

C_1, C_2 : Families of physical characteristics

C_m : Pressure coefficient

E : Modulus of Elasticity

F : $= \eta'(f_{k-1} + f_k)/4$

f : Nondimensional forcing function = Z^s_{tt}/g

G : Shear modulus

g : Acceleration due to gravity

H : Height of water in reservoir basin

I : Second moment of area about y-axis

I_o : Second moment of area about y-axis at base

$\bar{I}$: Nondimensional second moment of area about y-asix $= I/I_o$

J : Rotary inertia about y-axis

J_o : Rotary inertia at base about y-axis

$\bar{J}$: Nondimensional rotary inertia about y-axis $= J/J_o$

k : Shape factor

k_1 : Velocity of flexural wave $= \sqrt{EI_o/\rho^c J_o}$

k_2 : Velocity of shear wave $= \sqrt{kG/\rho^c}$

L : Height of the highest monolith of the dam

M : Bending Moment

$\bar{M}$: Nondimensional bending moment $= ML/EI_o$

r : Radius of gyration about y-axis

t : Time

V : Shear force

$\bar{V}$: Nondimensional shear force $= VL^2/EI_o$

$\bar{v}$: Nondimensional linear velocity $= w_t/k_2$

w : Displacement in z-direction

$\bar{w}$: Nondimensional displacement in z-direction $= w/L$

x : Distance from base

$\bar{x}$: Nondimensional distance from base = x/L

Z^{s}_{tt} : Ground acceleration

2. Greek Symbols

α : $= 1.0 + \rho^{w} A^{w} / \rho^{c} A^{c}$

β : $= \dfrac{2 \rho^{c} A_o L^3 k_2 \omega_f \mu}{EI_o}$

β' : $= \beta / c_2$

ξ : $= \dfrac{A_o L^2}{J_o} (k_2/k_1)^3$

λ : $= \dfrac{k_2 A_o L^2}{k_1 J_o}$

λ' : $= \lambda / c_2$

μ : Damping ratio

σ/E : Nondimensional bending stress

τ : Nondimensional time = $k_1 t/L$

ϕ : Angle of taper with x-axis

ψ : Bending slope

η : $= \dfrac{\rho^c \, g \, A_o \, L^3}{EI_o}$

η' : $= \eta / \omega_2$

ω_f : Fundamental frequency

ω_d : Damped frequency

ω_n : Natural frequency

ρ^c : Mass per unit volume of beam

ρ^w : Mass per unit volume of water

δ : Jump

3. Mathematical Symbols

$[\ ]$: Matrix

$\langle\ \rangle$: Row vector

$\{\ \}$: Column Vector

$|\ |$: Determinant

$\{\ \}^T$: Transpose of column vector

ABSTRACT

The transient stresses developed due to earthquake play a major role in the failure of structure due to dynamic loading. In this study integration along the characteristics of the resulting equations is used in numerical solution for the transient response of dam-like structure. The method is compared with known closed form solution and is found to be in good agreement.

The dam-like structure is treated firstly without water in reservoir basin and secondly with impounding water. The effect of water on the dam is taken into account by virtual mass addition. It is found that the maximum transient bending stresses developed in the dam are higher than those obtained by the usual mode superposition analysis.

This analysis is applied for the dynamic response of the highest monolith of the Koyna Dam subjected to December 11th (1967) earthquake. The method is equally applicable to the dynamic analysis of stacks subjected to earth motion.

CHAPTER I

INTRODUCTORY REMARKS

1.1 INTRODUCTION

An earthquake is a ground vibration phenomenon. The ground vibration associated with an earthquake is of random type i.e. the peaksof acceleration, both positive and negative, have various amplitudes and occur at various time intervals without any specific pattern. Structures situated on the ground are forced to respond to these motions and therefore set into vibration. An earthquake produces only ground vibration, therefore exerts forces only at the base of a structure. The forces induced in the structure at a higher level are developed as a result of dynamic response of the structure. During an earthquake the ground motion occurs in all directions horizontal and vertical. However, horizontal components are more important than vertical ones since the structure is usually strong enough in the vertical direction.

In general, three techniques are available for the theoretical analysis of transient stresses in elastic bodies caused by impact loadings such as earthquake. These methods are:

(i) The method of mode superposition

(ii) The Laplace transform technique

(iii) The method of characteristics.

The method of mode superposition is often unsatisfactory since it utilises the normal mode of vibration as predicted by the elementary theory and many modes are often required for rapid convergence of results. Also this technique tends to round off or average out the sharp peaks in the response.

The Laplace transform technique gives a solution of closed form type, hence it always demands a closed form representation of input motion during the total interval of disturbance. Moreover, this technique has its inherent inversion difficulties and frequently numerical method of integration has to be employed to evaluate inverse integral of the transform.

The advantages of the method of characteristics, employed in this study, are that, firstly, the problem can be formulated as continuous one i.e. no discretization of physical model is needed. Secondly, it gives a simple description of wavefronts and finally, well known technique of numerical integration can be effectively used.

1.2 HISTORICAL BACKGROUND

The method of characteristics was first used by Leonard and Budiansky [1]* to solve a strictly mathematical transient problem of a beam i.e. when the governing equations and initial conditions are homogeneous but the boundary conditions are nonhomogeneous. However, solutions were obtained for a particular type of material for which both shear and flexural wave have the same velocities of propagation. Subsequently Jhasman [2] obtained the relation between the various stresses and displacement derivatives at the wavefronts due to step inputs for circular sheets and plates following the same general principle of Leonard and Budiansky, but did not solve the characteristic equations behind the wave front. Later Plass [3] improved the problem of Leonard and Budiansky for material which posseses two different wave velocities but his inputs were such that there was no discontinuity along the slower wave fronts. Spillers [4] applied the method of characteristics to solve a semi-infinite cylindrical (Timoshenko type) shell subjected to dynamic loading at one end. His input was also such that there was no discontinuity along the slower wavefront. Subsequently Chou and Koenig [5] applied the method of characteristics for several spherical and cylindrical dilatation wave problems. Recently Chou and Mortimer [6] proposed an

---

* Numbers in parantheses represent reference in Appendix III

unified approach for one dimensional wave propagation problem where propagation of discontinuity along waves may exist. He proposed a method of solution for a system of n second order partial differential equations with generalised displacement as dependent variables.

1.3 OBJECT AND SCOPE OF THE STUDY

It is felt that a thorough knowledge of the transient stresses developed in a dam-like structure subjected to ground motion will be useful for the advancement of theoretical knowledge about the behaviour of such structure during an earthquake. For this study information from the records of a recent earthquake (11th December,1967) at Koyna, situated at the south-west end of the Deccan trap, have been used. The physical details of the dam at Koyna are used in the numerical example of this study. Analysis for the longitudinal component of horizontal strong motion is ignored since the dam is strong enough in longitudinal direction. To date, very few records of actual strong motion are available in this belt, and there is therefore little statistical basis for the prediction of further eqrthquakes. Hence, the result of the analysis predicts the transient stresses developed in Koyna-concrete-dam during earthquake on 11th December, 1967.

The problem is formulated in Chapter II. The governing equations considering the hydrodynamic effect are developed and characteristic equations as well as compatibility along the characteristics are established.

Recurrence relations for numerical step by step integration are given in Chapter III. Stability and convergence of numerical integration scheme are discussed.

Thirdly in Chapter IV, summary of the investigation is outlined and conclusions are drawn. A comparitive study of the effect of change of cross section of a cantilever beam for a particular input ground motion has also been conducted in this section. It is felt that analysis developed herein will help visualising the transient stresses developed in structure subjected to ground motion. The analysis presented herein will be useful for the analysis of tall stack-like structure under dynamic loading.

Details of the matrices, determinants and vectors introduced in Chapter II and Chapter III are given in Appendix I.

Finally in Appendix II, propagation of discontinuities in the domain of solution are discussed. The equation of jump across wavefronts are developed. Details of the problem solved by Leonard and Budiansky [1] are also given here.

CHAPTER II

FORMULATION OF PROBLEM

2.1 BASIC EQUATIONS, INITIAL AND BOUNDARY CONDITIONS

Concrete gravity dams are generally cast in monoliths. The joint between two subsequent monoliths are packed with waterproof materials to prevent waterleakage. For reduction of thermal stresses in the structure it is customary to avoid any interconnection of two adjacent monoliths (Figure 1). After the earthquake on 11th December, 1967 independent deformation of adjacent monoliths of Koyna-concrete dam had been noticed clearly. Hence, the dam can be assumed for analysis as a cantilever beam with distributed mass, according to the cross section of dam, along the height of the dam for a particular monolith. Since monolith has considerable width in transverse direction compared to the height of dam, shear deformation cannot be neglected. Rotation of the cross section of dam will be small. However, for accuracy of analysis correction for rotation has been considered.

General assumotion for the material of the dam and impounding water are the followings:

(1) The material of the dam (concrete) is linearly elastic

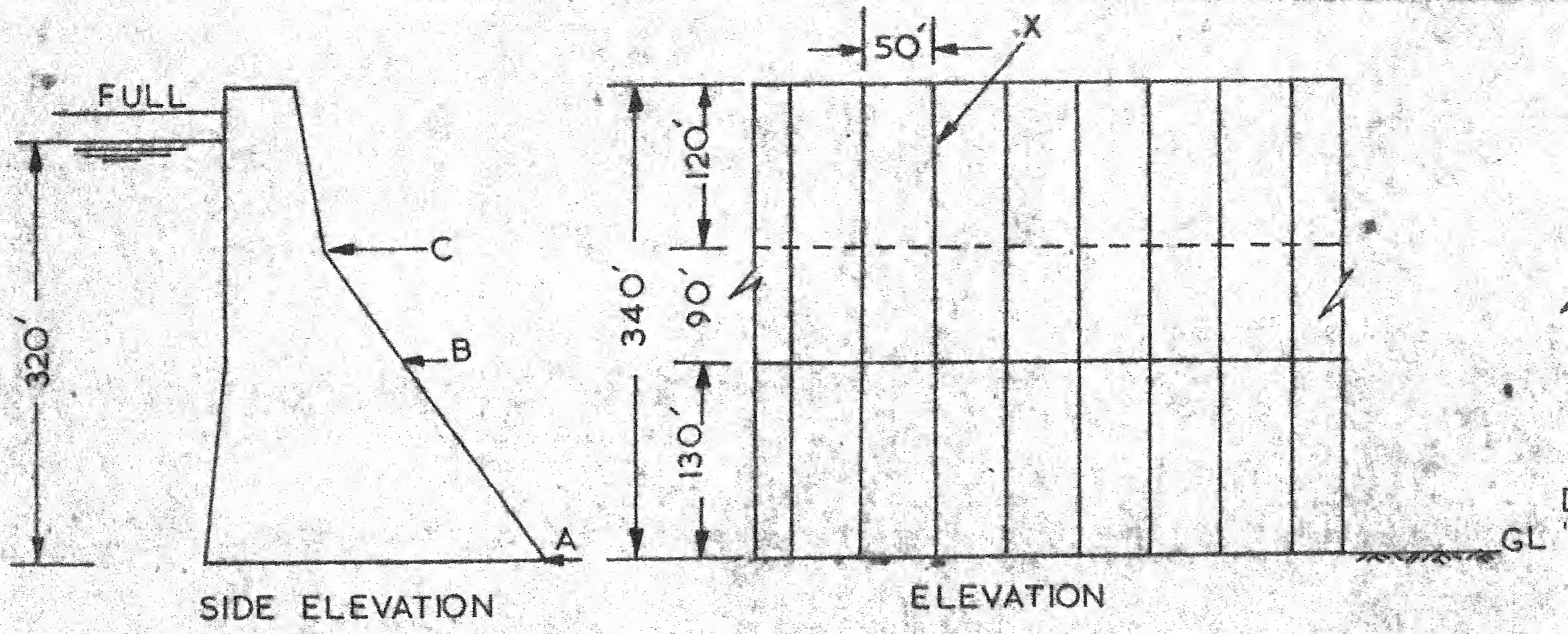

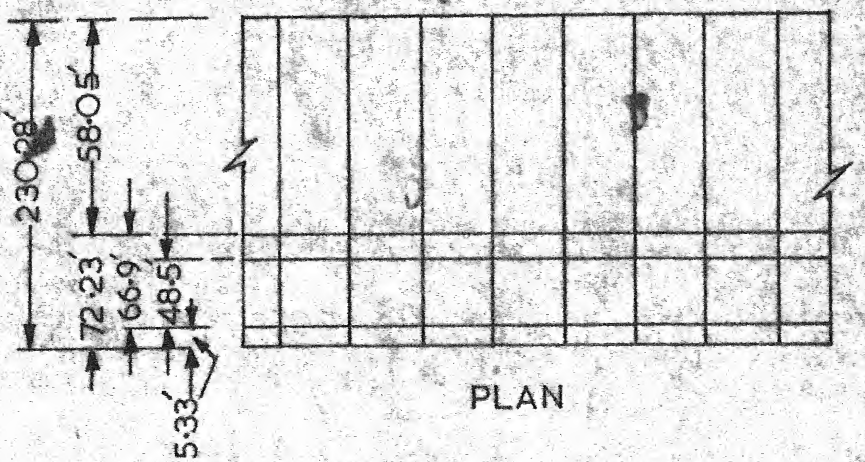

NOTE
DRAWING NOT IN SCALE

FIG. I STRUCTURAL DETAILS OF DAM

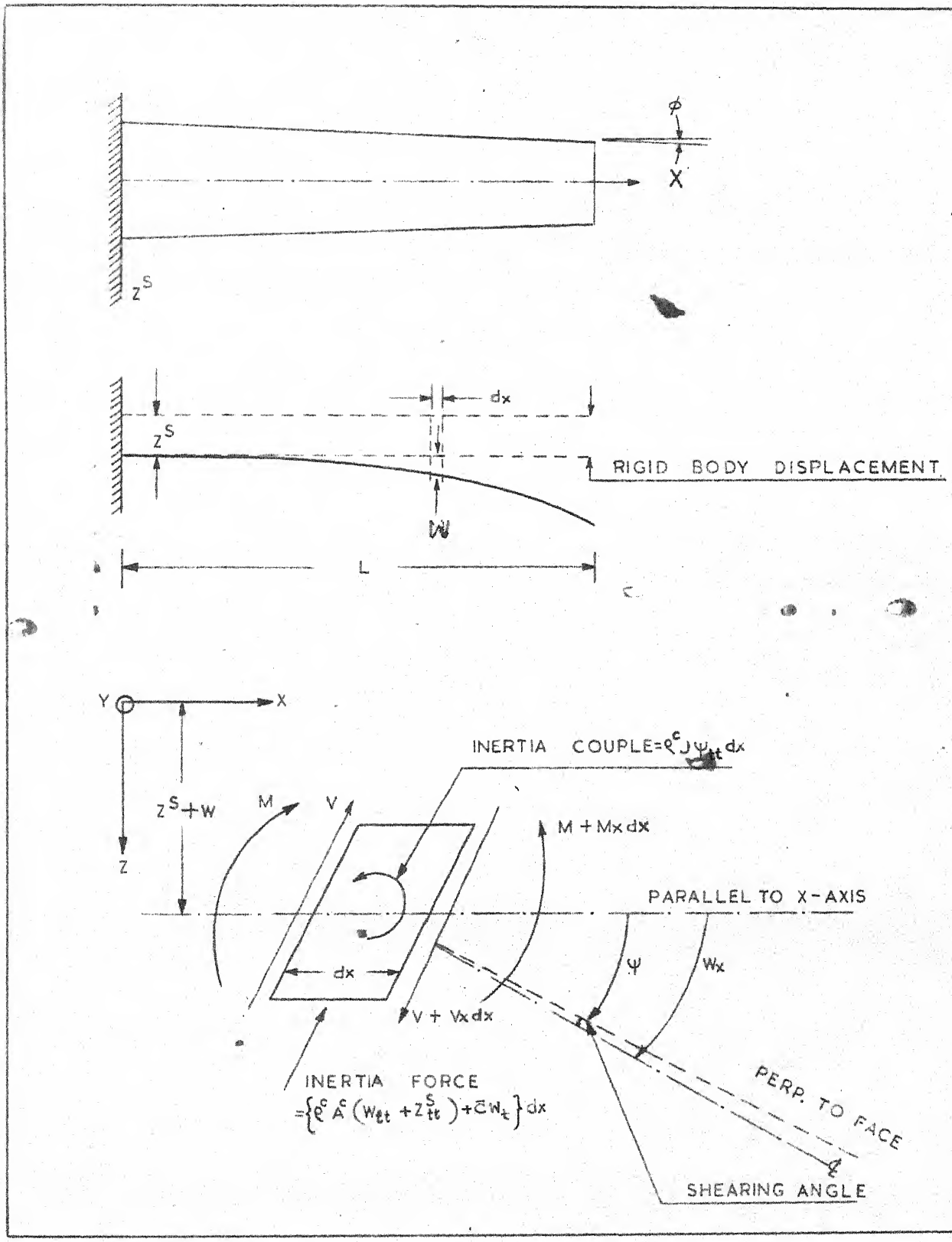

FIG·2 FORCE ACTING ON AN ELEMENT OF BEAM.

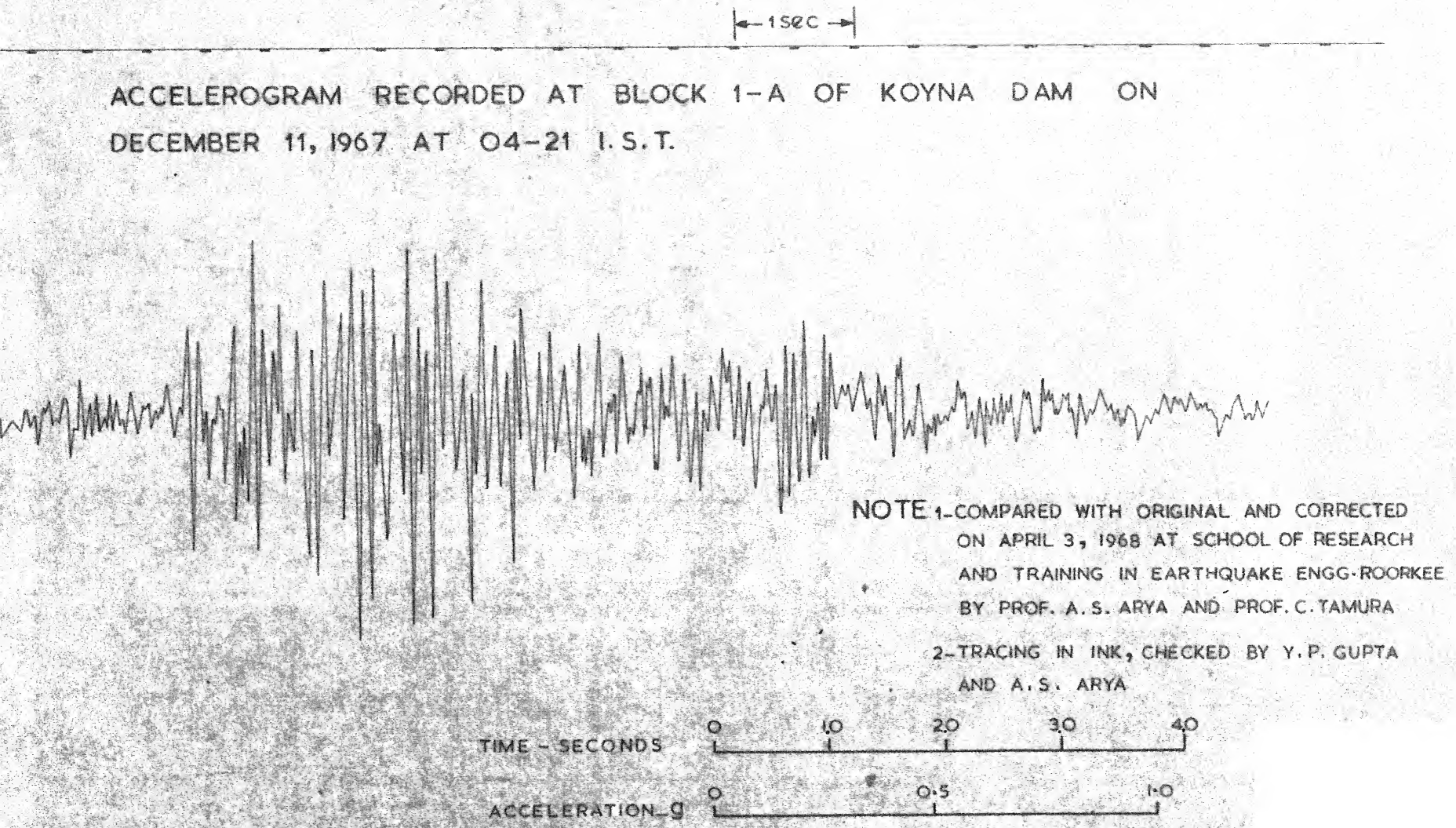

FIG.3 HORIZONTAL COMPONENT TRANSVERSE TO DAM AXIS

with viscous damping proportional to a constant β which varies, for concrete, from 0.1 to 0.15 times the fundamental critical damping C. Fundamental critical damping corresponds to the limiting case of periodic oscillation involving deformation of all the masses toward the same side and can be written as:

$$\text{Fundamental critical damping } C = 2 \rho^c A^c \omega_f \qquad (2.1)$$

where, ρ^c = density of concrete

A^c = area of concrete at a particular cross section of monolith.

ω_f = fundamental frequency of the system.

(ii) Effect of crack in the concrete is neglected.

(iii) The impounding water is incompressible with irrotational flow of small amplitude. The internal viscosity and some other causes of energy dissipation from the impounding water are disregarded, as well as the effect of surface wave.

2.1.1 Equation of Vibration of Beam

Assuming relative deflection w from the support and rotation ψ of the cross section to be small the dynamic equilibrium of Timoshenko beam (Figure 2), subjected to

ground acceleration Z^s_{tt}(Figure 3), including the effect of the rotary inertia and the shear deformation may be given as the followings:

$$M + EI\,\psi_x = 0 \tag{2.2}$$

$$V - kA^cG(w_x - \psi) = 0 \tag{2.3}$$

$$M_x + \rho^c J\,\psi_{tt} - V = 0 \tag{2.4}$$

$$V_x - \rho^c A^c(w_{tt} + Z^s_{tt}) - \bar{C}\,w_t = 0 \tag{2.5}$$

where

$\bar{C} = \mu C$

J = rotary inertia about y-axis.

Other symbols are used in standard form.

In the set of Equations (2.2 to 2.5) subscripts refer to the partial differentiation with respect to variables mentioned there.

For a cantilever beam subjected to sudden ground acceleration the initial condition can be written as:

$$w(x,0) = w_t(x,0) = \psi(x,0)$$

$$= \psi_t(x,0) = 0 \tag{2.6}$$

and the boundary conditions are

$$M(L,t) = V(L,t) = w(0,t) = \psi(0,t) = 0 \qquad (2.7)$$

System of Equations (2.2 to 2.5) represents dynamic equilibrium of a monolith of dam subjected to an earthquake where reservoir basin has no impounding water with initial conditions (Equation 2.6) and boundary conditions (Equation 2.7).

2.1.2 Governing Equation of Monolith of Dam Vibration With Effect of Water in the Reservoir Basin

Hydrodynamic pressure will develop on the upstream face of a dam during an earthquake in opposite phase with ground acceleration. Hence, equivalent inertia force of the mass of moving water with the dam is to be added with the inertia force of dam itself. The width of water b moving with the dam during an earthquake in accordance with Zanger's [7] theory is given by

$$b = \frac{C_m H}{2}\left[\left(1 - \frac{x^2}{H^2}\right) + \left(1 - \frac{x^2}{H^2}\right)^{1/2}\right] \qquad (2.8)$$

where

x = height of particular cross-section from the base of the dam

H = height of impounding water at upstream of the dam

C_m = pressure coefficient depending on the angle of inclination of the upstream face with vertical.

Hence, mass of the water along per foot width of the dam is given by,

$$\text{mass/ft} = \rho^w A^w = \rho^w b \qquad (2.9)$$

since unit width in the longitudinal direction is considered in this analysis. In Equation (2.9)

ρ^w = density of water

A^w = area of water

Neglecting the hydrodynamic effect due to deformation of dam, the governing differential equation of dynamic equilibrium of the monolith of a dam may be given by system of Equations (2.2) to (2.4) and

$$V_x - \rho^c A^c w_{tt} - \bar{C} w_t - \rho A Z^s_{tt} = 0 \qquad (2.10)$$

where

$$\rho A = \rho^c A^c + \rho^w A^w$$

The system of Equations (2.2 to 2.4) and Equation (2.10) are the governing equations with initial conditions (Equation 2.6) and boundary conditions (Equation 2.7) for

the vibration of a monolith of dam subjected to an earthquake.

2.2 DERIVATION OF COMPATIBILITY CONDITION

The input acceleration for response in the structure due to an earthquake is a seismograph reading and it is difficult to obtain any closed form representation of the same. Hence numerical solution of the problem will be sought in this study. To facilitate numerical integration in continuous formulation, it is advantageous to change the system of Equations (2.2) to (2.4) and(2.10) along with initial conditions (2.6) and boundary conditions (2.7) in a physical plane (x,t-plane) to the characteristic form.

Differentiation of equation (2.2) and (2.3) with resp ct to t yields

$$M_t + EI\,\psi_{xt} = 0 \qquad (2.11)$$

$$V_t - kA^cG(w_{xt} - \psi_t) = 0 \qquad (2.12)$$

Equations(2.11), (2.12), (2.4) and (2.10) form a system of four simultaneous partial differential equations which in the non-dimensional form are given as:

$$\bar{M}_{\bar{\zeta}} + \bar{I}\,\bar{a}_{\bar{x}} = 0 \qquad (2.13)$$

$$\frac{\bar{V}_{\bar{\zeta}}}{\xi\,\bar{A}} - \bar{v}_{\bar{x}} + \frac{k_1}{k_2}\,\bar{a} = 0 \qquad (2.14)$$

$$\bar{M}_{\bar{x}} + \bar{J}\,\bar{a}_{\tau} - \bar{V} = 0 \qquad (2.15)$$

$$\frac{\bar{V}_{\bar{x}}}{\bar{A}} - \lambda\bar{v}_{\tau} - \beta\bar{v} - \gamma\alpha f = 0 \qquad (2.16)$$

where

$\bar{A}$ = nondimensional area = $\frac{A^c}{A_o^c}$

k_1 = propagation velocity of the flexural wave

= $\left(\frac{EI_o}{\rho^c J_o}\right)^{1/2}$

k_2 = propagation velocity of shear wave = $\left(\frac{kG}{\rho^c}\right)^{1/2}$

τ = nondimensional time = $\frac{k_1 t}{L}$

$\bar{a}$ = nondimensional angular velocity = Ψ_{τ}

$\bar{v}$ = nondimensional linear velocity = $\frac{k_1}{k_2}\bar{w}_{\tau}$

$f = Z^s_{tt}/g$

λ, γ, α and β are nondimensional parameter and all barred quantities are nondimensional form of unbarred quantities.

The nondimensional parameter $\alpha = 1.0$ when there is no water in reservoir basin or when hydrodynamic effect of water is neglected and $\alpha = 1.0 + \rho^w A^w / \rho^c A^c$ for vibration of monolith of dam with a reservoir basin of water.

The initial conditions given by Equation (2.6) change to

$$\bar{w}(\bar{x},0) = \bar{v}(\bar{x},0) = \psi(\bar{x},0)$$

$$= \bar{a}(\bar{x},0) = 0 \qquad (2.17)$$

and the boundary conditions (Equation 2.7) in nondimensional form are

$$\bar{M}(1,\tau) = \bar{V}(1,\tau) = \bar{w}(0,\tau)$$

$$= \psi(0,\tau) = 0 \qquad (2.18)$$

A characteristic direction of the system of Equations (2.13 to 2.16) allow possible discontinuity of the first derivative of dependent variables ($\bar{a}$, $\bar{v}$, $\bar{M}$, $\bar{V}$) along its normal direction. Given initial data on such a direction the normal derivative of the variables are not uniquely determined by the system of Equations (2.13 to 2.16). However, for regions in $\bar{x}$, τ -plane where the dependent variables are continuous the following relation must be satisfied:

$$d\bar{M} = \bar{M}_{\bar{x}}\, d\bar{x} + \bar{M}_{\tau}\, d\tau \qquad (2.19)$$

$$d\bar{a} = \bar{a}_{\bar{x}}\, d\bar{x} + \bar{a}_{\tau}\, d\tau \qquad (2.20)$$

$$d\bar{v} = \bar{v}_{\bar{x}}\, d\bar{x} + \bar{v}_{\tau}\, d\tau \qquad (2.21)$$

$$d\bar{V} = \bar{V}_{\bar{x}}\, d\bar{x} + \bar{V}_{\tau}\, d\tau \qquad (2.22)$$

Equations (2.13 to 2.16 and 2.19 to 2.22) form a system of eight equations which may be used to solve for eight first derivatives of dependent variables if the distribution of dependent variables are known along an initial curve. The system of Equations (2.13 to 2.16 and 2.19 to 2.22) can be given in matrix form:

$$[X] \{Z\} = \{W\} \tag{2.23}$$

where

$[\,]$ → represents a matrix

$\{\,\}$ → represents a vector

The matrix X, vectors W and Z are given in Appendix I.

Solving for $\bar{M}_\tau$ from Equation (2.23) by well known Cramer's rule yields

$$\bar{M}_\tau = \frac{|Y|}{|X|} \tag{2.24}$$

where

$|\,|$ → represents a determinant.

$|Y|$ is formed by replacing one column of $[X]$ by $\{W\}$ according to Cramer's Rule.

Since first derivative of dependent variables may be discontinuous, the derivative $\bar{M}_\tau$ is undetermined. A necessary and sufficient condition for the indeterminacy of

$\bar{M}_\tau$ is $|X| = 0$ and $|Y| = 0$. The vanishing of $|X|$ leads after applying Laplace expansion technique of determinants to:

$$\left[\bar{I}(d\tau)^2 - \bar{J}(d\bar{x})^2\right]\left[\frac{\lambda}{\xi_3 \bar{A}} - \frac{1}{\bar{A}}(d\tau)^2\right] = 0 \tag{2.25}$$

Therefore, either

$$\frac{d\tau}{d\bar{x}} = \pm (\bar{J}/\bar{I})^{1/2} = \pm C_1 \tag{2.26}$$

or

$$\frac{d\tau}{d\bar{x}} = \pm (\lambda/\xi_3)^{1/2} = \pm C_2 \tag{2.27}$$

Hence the original system of Equations (2.2 to 2.4 and 2.10) are totally hyperbolic since the roots of Equation (2.25) are real and distinct. The roots $\pm C_1$ ($1 = 1,2$) are called physical characteristic direction and it is customary to call inverse of it as the wave velocity.

The vanishing of $|Y|$ yields, the characteristic equation where $d\tau/d\bar{x}$ is replaced by $\pm C_1$

$$\bar{V}d\tau - \bar{J}\, d\bar{a} \mp C_1\, d\bar{M} = 0 \tag{2.28}$$

The equation (2.28) will be called compatibility relation along $+C_1$ and $-C_1$ respectively. It can be very

easily shown solving for either $\bar{M}_{\bar{x}}$ or $\bar{a}_{\bar{\tau}}$ or $\bar{a}_{\bar{x}}$ will result in sets of equation which are identical to Equation (2.26) and Equation (2.28).

Similarly solving for $\bar{V}_{\bar{\tau}}$ or $\bar{V}_{\bar{x}}$ or $\bar{v}_{\bar{\tau}}$ or $\bar{v}_{\bar{x}}$ will lead to the identical equation-compatibility relation along $\pm C_2$. After replacing $d\bar{\tau}/d\bar{x}$ by $\pm C_2$ the compatibility relation along $\pm C_2$ are given as:

$$\left[-\lambda' \bar{a} \pm \eta' \alpha f \pm \beta' \bar{v} \right] d\bar{\tau} \pm \lambda' d\bar{v} - \frac{d\bar{V}}{\bar{A}} = 0 \qquad (2.29)$$

where

$$\lambda' = \frac{\lambda}{C_2}$$

$$\beta' = \frac{\beta}{C_2}$$

$$\eta' = \frac{\eta}{C_2}$$

Solution of the dependent variables may be obtained in the region, where the dependent variables are continuous, by solving the system of four Equations (2.28 to 2.29) simultaneously along the characteristic directions (Equation 2.26 and 2.27) with proper initial conditions (Equation 2.17) and boundary conditions (Equation 2.18).

CHAPTER III

NUMERICAL SOLUTION

3.1 DERIVATION OF RECURRENCE RELATION

Solution of the system of equations (2.26 to 2.29) can be obtained numerically by step by step integration which amounts to marching out of solution from $\tau = 0$ by means of Hartree [8] technique of numerical integration. In performing numerical integration, the finite length in the $\bar{x}$ direction is divided by strips at an interval h (J - 1, J, J + 1 etc. in Figure 4) which inturn form a mesh network with the constant time line (K - 1, K, K + 1 etc. in Figure 4). The dependent variables ($\bar{a}$, $\bar{v}$, $\bar{V}$, $\bar{M}$), in this process, are considered as known functions of $\bar{x}$ at a time τ, either as given initial conditions or as the output of previous stage computations.

Let the dependent variables be known on a line $\tau = \tau_1$ and is required to be found on a line $\tau = \tau_1 + \Delta\tau$ on which a typical pivotal point is J, K (Figure 4). There are four families of characteristics ($\pm C_1$ and $\pm C_2$) passing through each interior pivotal point (grid). These families of characteristics intersect the initial line K-1 at four points (I-1, I-2, I+1, and I+2 in Figure 4) - which hence-forth will be called subgrids. Since coordinates of pivotal

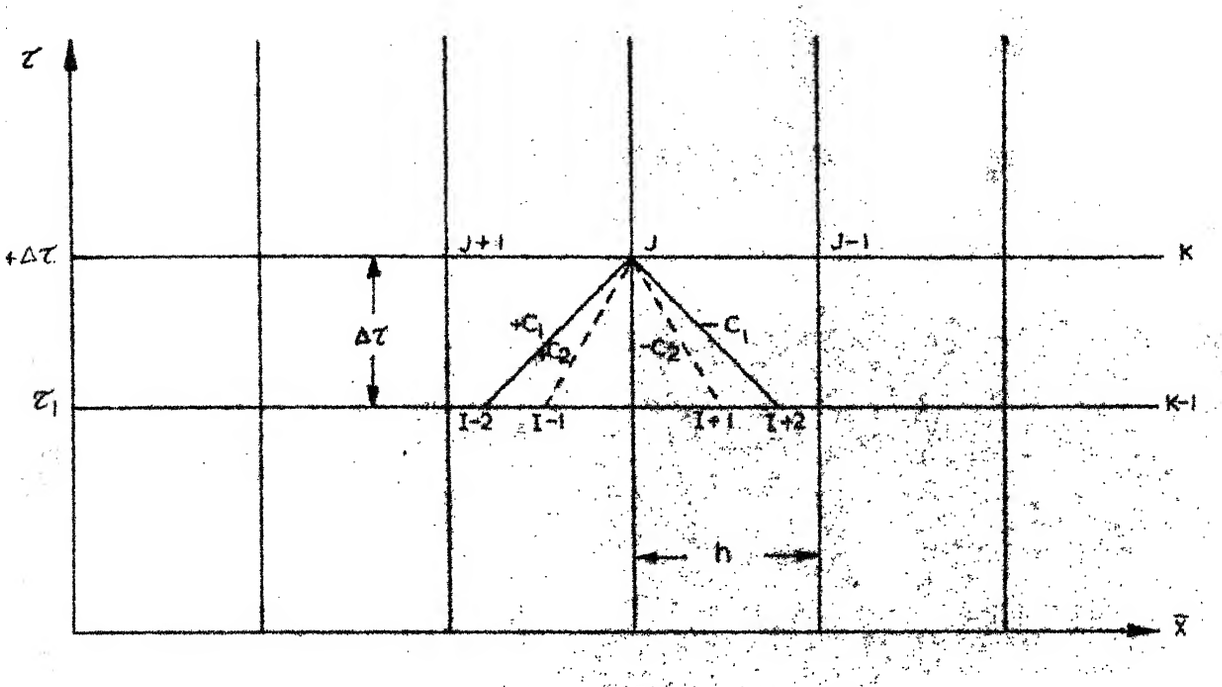

FIG. 4 INTERIOR GRIDS

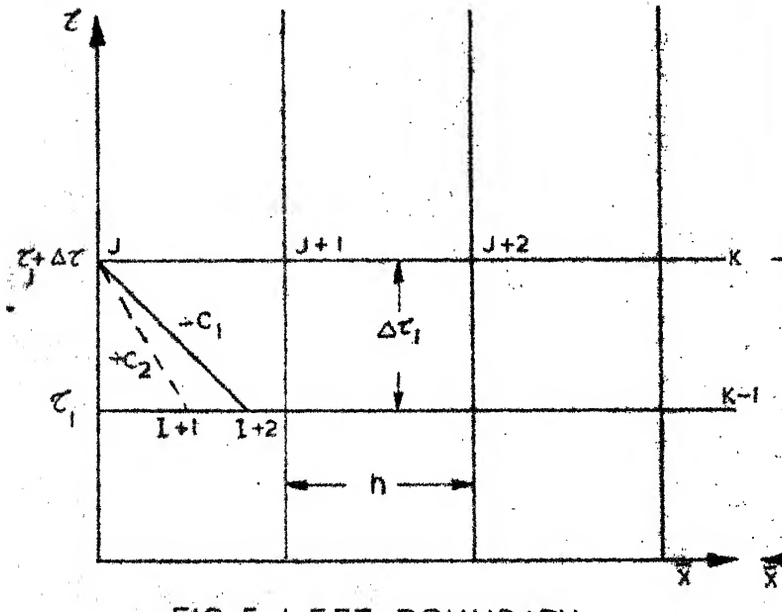

FIG. 5 LEFT BOUNDARY

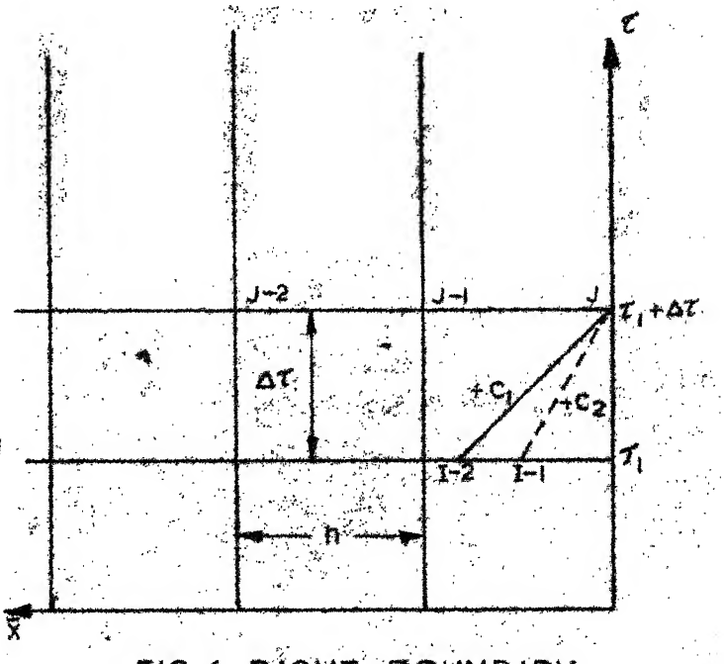

FIG. 6 RIGHT BOUNDARY

point J,K is known, using Equation (2.26) and Equation (2.27) space coordinate $\bar{x}$ of subgrids may be obtained.

Equation (2.26) in finite difference form reduces to:

$$\bar{x}_{I-2} = \bar{x}_J - \Delta\tau/C_1 \qquad (3.1)$$

$$\bar{x}_{I+2} = \bar{x}_J + \Delta\tau/C_1 \qquad (3.2)$$

Since C_1 is the slope of the characteristic line and for a rectangular cross section (I = J) it has a constant slope.

Similarly, Equation (2.27) yields

$$\bar{x}_{I-1} = \bar{x}_J - \Delta\tau/C_2 \qquad (3.3)$$

and $$\bar{x}_{I+1} = \bar{x}_J + \Delta\tau/C_2 \qquad (3.4)$$

In equations (3.1 to 3.4) subscripts refer to the subgrids or grids.

Since the dependent variables ($\bar{a}$, $\bar{v}$, $\bar{M}$, $\bar{V}$) are known functions at three adjacent main grid points (J, J-1 and J+1 in Figure 4) on the initial line K-1, knowing the coordinates of m^{th} subgrid a quadratic interpolation formula as given below may be used to find each of the variables.

$$\bar{a}_{m,k-1} = \bar{a}_{J,k-1} - \frac{\bar{x}_J - \bar{x}_m}{2h}(\bar{a}_{J+1,k-1} - \bar{a}_{J-1,k-1}) + \frac{(\bar{x}_J - \bar{x}_m)^2}{2h^2}(\bar{a}_{J+1,k-1} - 2\bar{a}_{J,k-1} + \bar{a}_{J-1,k-1}) \tag{3.5}$$

where $\bar{a}_{J+1,k-1}$ refers to the functional value of $\bar{a}$ at grid point J+1 and on the line K-1 and $\bar{x}_J$ refers to the space coordinate of J. The nomenclature introduced will be used hereafter in this study.

Formulae similar to Equation (3.5) can be written easily for the remaining dependent variables.

For a particular pivotal point J, K the compatibility relations (equations 2.28 and 2.29) are written in finite difference form in terms of the known values of dependent variables at subgrids.

Equation (2.28) replaced by finite difference gives

along $+C_1$:

$$\frac{1}{2}(\bar{V}_{J,k} + \bar{V}_{I-2,k-1})\,d\tilde{} - \frac{1}{2}J_{I-2}(\bar{a}_{J,k} - \bar{a}_{I-2,k-1}) - C_1(\bar{M}_{J,k} - \bar{M}_{I-2,k-1}) = 0 \tag{3.6}$$

and along $-C_1$:

$$\frac{1}{2}(\bar{V}_{J,k} + \bar{V}_{l+2,k-1})d\tau - \frac{1}{2}J_{l+2}(\bar{a}_{J,k} - \bar{a}_{l+2,k-1})$$

$$+ C_1(\bar{M}_{J,k} - \bar{M}_{l+2,k-1}) = 0 \qquad (3.7)$$

where

$$J_{l+2} = \bar{J}_J + \bar{J}_{l+2}$$

and $$J_{l-2} = \bar{J}_J + \bar{J}_{l-2}$$

Similarly Equation (2.29) reduces to

along $+C_2$:

$$-\frac{\lambda'}{2}(\bar{a}_{J,k} + \bar{a}_{l-1,k-1})d\tau + (\lambda' + \frac{\beta' d\tau}{2})\bar{v}_{J,k}$$

$$-(\lambda' - \frac{\beta' d\tau}{2})\bar{v}_{l-1,k-1} - \frac{2}{A_{l-1}}(\bar{V}_{J,k} - \bar{V}_{l-1,k-1})$$

$$= -F(\alpha_J + \alpha_{l-1})d\tau \qquad (3.8)$$

and along $-C_2$:

$$-\frac{\lambda'}{2}(\bar{a}_{J,k} + \bar{a}_{l+1,k-1})d\tau - (\lambda' + \frac{\beta' d\tau}{2})\bar{v}_{J,k}$$

$$+(\lambda - \frac{\beta' d\tau}{2})\bar{v}_{l+1,k-1} - \frac{2}{A_{l+1}}(\bar{V}_{J,k} - \bar{V}_{l+1,k-1})$$

$$= F(\alpha_J + \alpha_{l+1})d\tau \qquad (3.9)$$

where

$$A_{l-1} = \bar{A}_J + \bar{A}_{l-1}$$

$$\bar{A}_{I+1} = \bar{A}_J + \bar{A}_{I+1}$$

and $$F = \gamma_J'(f_{k-1} + f_k)/4$$

The f_k refers to ground acceleration at time $\tau = K$ and α_J refers to value of the same at grid or subgrid mentioned in subscript.

In writing Equations(3.6 to 3.9) it is assumed that $\Delta\tau$ is sufficiently small so that linear relation holds between the pivotal point and initial line and hence, averaging of dependent variables may be done.

The system of Equations (3.6 to 3.9) may be written in matrix notation as the following:

$$[B] \{U\} = [C] \{P\} + \{Q\} \qquad (3.10)$$

where

$[B]$ and $[C]$ = Coefficient matrix

$\{U\}$ = vector of the dependent variables at pivolal point J,K.

$\{P\}$ = vector representing dependent variables at subgrids

$\{Q\}$ = vector of input ground acceleration.

Equation (3.10) may be reduced to give a recurrence relation for step by step integration for pivotal mesh point

as encountered, which is given by

$$\{U\} = [B]^{-1} [C] \{P\} + [B]^{-1} \{Q\} \qquad (3.11)$$

where

$[B]^{-1}$ = inverse of $[B]$.

Details of all vectors and matrices used in Equation (3.11) are given in Appendix I.

For the vertical boundary plane ($\bar{x} = 0$ and $\bar{x} = 1$) suitable recurrence relation may be obtained using proper boundary conditions and following the same general principle of interior mesh point. At the left boundary where $\bar{x} = 0$ (Figure 5) two families of characteristics ($- C_1$ and $- C_2$) intersect the boundary pivotal point J,K where the boundary conditions from Equation (2.18) are

$$\bar{a}(0, \bar{\tau}) = \bar{v}(0, \bar{\tau}) = 0$$

The space coordinate of subgrids (I+1 and I+2) may be obtained from Equation (3.2) and Equation (3.4). From known values of dependent variables at initial line, the functional value of variables at any subgrid m may be obtained by using an interpolation formula as the following

$$\bar{V}_{m,k-1} = \bar{V}_{J+1,k-1} - \frac{\bar{x}_{J+1} - \bar{x}_m}{2h}(\bar{V}_{J+2,k-1} - \bar{V}_{J,k-1}) + \frac{(\bar{x}_{J+1} - \bar{x}_m)^2}{2h^2}(\bar{V}_{J+2,k-1} - 2\bar{V}_{J+1,k-1} + \bar{V}_{J,k-1}) \qquad (3.12)$$

Formulae similar to Equation (3.12) may be used for remaining dependent variables. Introduction of known boundary conditions in finite difference form of compatibility relation along - C_1 and - C_2 yields:

along - C_1.

$$\frac{1}{2}(\bar{V}_{J,k} + \bar{V}_{I+2,k-1})d\tau + \frac{1}{2} J_{I+2}\, \bar{a}_{I+2,k-1} + C_1(\bar{M}_{J,k} - \bar{M}_{I+2,k-1}) = 0 \qquad (3.13)$$

and along - C_2:

$$-\frac{\lambda'}{2}\bar{a}_{I+1,k-1}\, d\tau + (\lambda' - \frac{\beta' d\tau}{2})\bar{v}_{I+1,k-1} - \frac{2}{A_{I+1}}(\bar{V}_{j,k} - \bar{V}_{I+1,k-1}) = F(\alpha_J + \alpha_{I+1})d\tau \qquad (3.14)$$

A recurrence relation for left boundary may be obtained solving Equation (3.13) and Equation (3.14) simultaneously and given by.

$$\begin{Bmatrix} \bar{V} \\ \bar{M} \end{Bmatrix}_{J,k} = [D]^{-1}\,[H]\,\{R\} + [D]^{-1}\,\{S\} \qquad (3.15)$$

where

$\begin{Bmatrix} \bar{V} \\ \bar{M} \end{Bmatrix}_{J,k}$ = vector of dependent variables as specified at pivotal point J,K

$\{R\}$ = vector of dependent variables at subgrids

$\{S\}$ = vector of the input ground acceleration

$[D]$ and $[H]$ are coefficient matrices.

Details of matrices and vectores used in Equation (3.15) are given in Appendix I.

Similarly for right boundary $\bar{x} = 1$ (Figure 6), where boundary conditions from (2.18) are

$$\bar{M}(1,\tau) = \bar{V}(1,\tau) = 0$$

The space coordinate of subgrids are found from Equation (3.1) and Equation (3.3). Dependent variables at m^{th} subgrid may be evaluated from the quadratic interpolation formula as given in the following:

$$\bar{a}_{m,k-1} = \bar{a}_{J-1,k-1} + \frac{\bar{x}_{J-1} - \bar{x}_m}{2h}(\bar{a}_{J,k-1} - \bar{a}_{J-2,k-1}) + \frac{(\bar{x}_{J-1} - \bar{x}_m)^2}{2h^2}(\bar{a}_{J,k-1} - 2\bar{a}_{J-1,k-1} + \bar{a}_{J-2,k-1}) \qquad (3.16)$$

Formulae similar to Equation (3.16) may be used for other dependent variables.

A recurrence relation similar to Equation (3.15) may be obtained by substituting proper boundary conditions in Equations (3.6)and Equation (3.8) and is given by:

$$\begin{Bmatrix} \bar{a} \\ \bar{v} \end{Bmatrix}_{J,k} = [W]^{-1} [N] \{T\} + [W]^{-1} \{L'\} \qquad (3.17)$$

where

$[W]$ and $[N]$ = coefficient matrices

$\begin{Bmatrix} \bar{a} \\ \bar{v} \end{Bmatrix}_{J,k}$ = dependent variable vector at pivotal point J,K

$\{T\}$ = vector of dependent variables at subgrids

and $\{L'\}$ = vector of ground acceleration.

Details of matrices and vector used in Equation (3.17) are given in Appendix I.

The solution of the set of Equations (2.26 to 2.29) may be obtained using the recurrence relations (Equations 3.10 , 3.15 and 3.17) and proper initial conditions (Equation 2.17).

3.2 STABILITY AND CONVERGENCE

To illustrate the general uniqueness theorem [9] of linear hyperbolic system of equations, let Γ_1 be a non-characteristic line (Figure 7) of continuous slope along which the dependent variables are prescribed as continuous functions. A unique solution to the system of equations (2.2 to 2.4 and 2.10) may be obtained in the triangular region Γ_P cut out by the outer characteristics ($\pm C_1$) at an interval $\Delta\tau$ from Γ_1 and having an intercept P_1P_4 on it. The interval P_1P_4 on the line Γ_1 is the domain of dependence of P on Γ_1. Hence, it is implied that the ratio of step size ($\Delta\tau / \Delta\bar{x}$) should comply with the outer characteristics.

The stability of finite difference scheme with rectangular grids was studied by Courant, Freidrichs and Lewy [10] for a wave equation ($u_{\bar{x}\bar{x}} = u_{\tau\tau}$) and the condition of stability and convergence towards the analytical solution as $\Delta\bar{x}$ and $\Delta\tau$ approach zero was found to be

$$\frac{\Delta\tau}{\Delta\bar{x}} \leqslant 1 \qquad (3.18)$$

In the case of wave equation, characteristics are two lines ($d\tau/d\bar{x} = \pm 1 = \pm C_1$) and the domain of dependence of P is Γ_P (Figure 8). So, if a step size is chosen

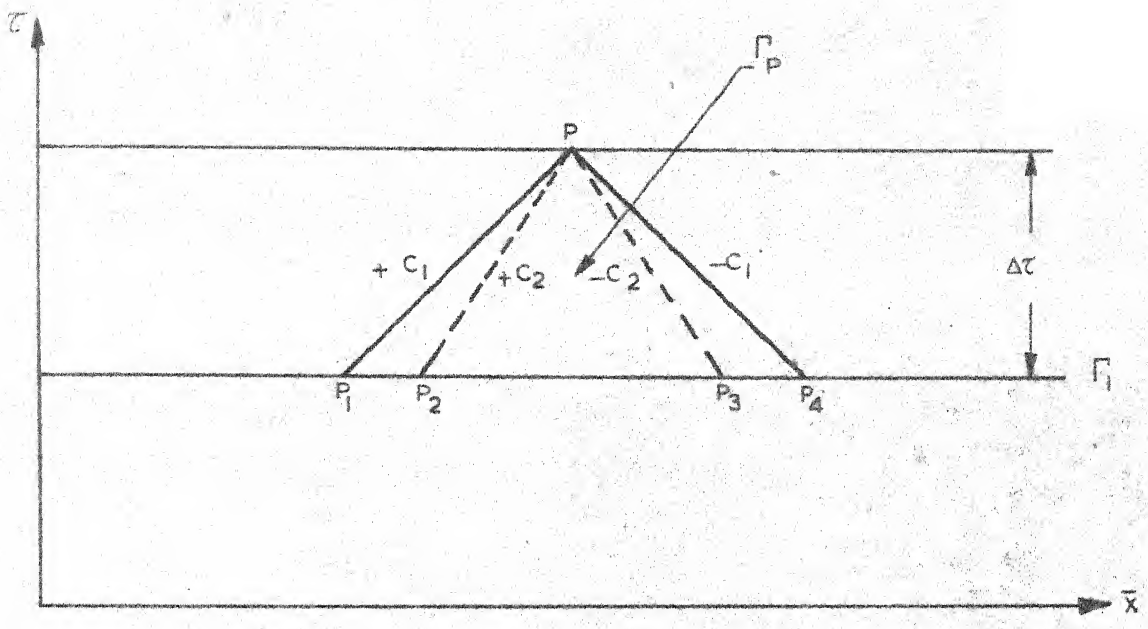

FIG. 7. DOMAIN OF DEPENDENCE

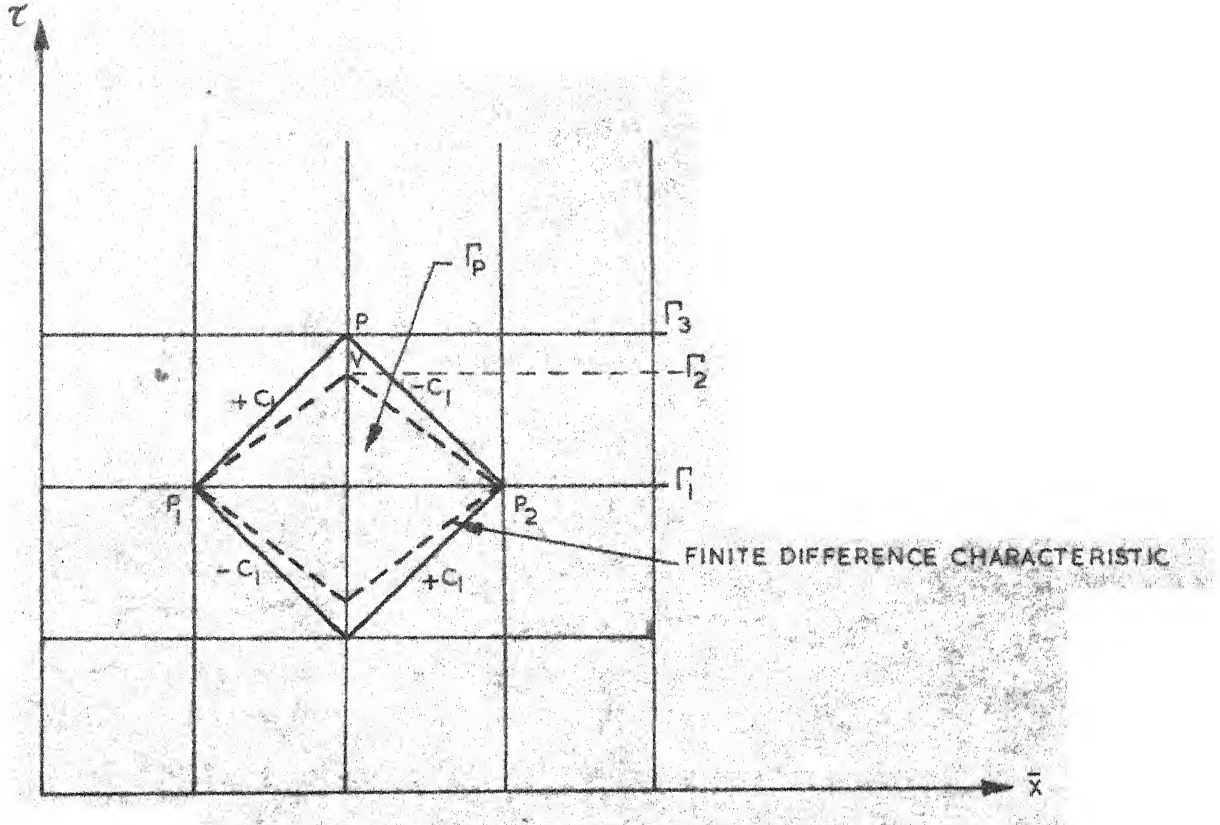

FIG. 8. CHARACTERISTIC FOR WAVE EQUATION

such that $\Delta\tau / \Delta\bar{x} > 1$, the pivotal point V then lies beyond the domain of dependence τ_p reached by the continuous solution. Hence, such a solution will hardly converge to the analytical one. However, accuracy of the solution is identical with the analytical one when $\Delta\tau / \Delta\bar{x} = 1$ since in this case pivotal point coincides with P. Accuracy of solution will decrease with decreasing ratio of step size owing to decrease of slope of the lines VP_1 and VP_2 which play the role of finite difference characteristics. However, a physical interpretation can also be given very easily. If for instance, the step size is taken less than the inverse of the faster wave velocity, it only amounts to artificial faster propagation of the wave. Hence, a step size is to be chosen as to comply with faster wave velocity for convergence of solution to the analytical one.

The proof of convergence of the Hartree scheme was also given by Sauer [11] in 1952.

5.5 NUMERICAL INTEGRATION

The height of the dam is divided by main grids at equal interval ($d\bar{x} = h$). The step size in τ direction is always chosen according to Equation (2.26). During integration, it is assumed that the accelerogram reading is linear between one peak to subsequent peak. The time interval between subsequent peaks is divided in n equal parts of

step size h and remaining portion $\Delta\tau$ forms another step. Hence, n+1 steps are required for integration of one peak to other. The procedure for step by step integration when $d\tau = d\bar{x} = h$ can be summarised as follows:

Step (1):

The space coordinate of subgrids are located using Equations (3.1 to 3.4).

Step (2):

Since $C_1 = 1$ for the problem, the dependent variables at interior subgrids (Figure 4) I+1 and I-1 are interpolated from the known variables at main grids on initial line using suitable interpolation formula similar to Equation (3.5) or Equation (3.12) or Equation (3.15).

Step (3):

Dependent variables at main grids are then calculated using suitable recurrence relations from Equation (3.10, 3.15 and 3.17).

For the last step $\Delta\tau$ step (1) and step (2) remain identical except step (2) where variables at all subgrids have to be interpolated.

By continuously repeating the basic computational steps the solution may be marched out from $\tau = 0$. However, for starting integration at $\tau = 0$ initial conditions (Equation 2.17) have to be used.

CHAPTER IV

DISCUSSION AND CONCLUSION

4.1 DISCUSSION ON NUMERICAL ANALYSIS

Stability and convergence of the numerical scheme proposed in this study has been discussed in Chapter III. The validity of the seheme is shown by comparing the results obtained for a problem with a known closed-form solution. The convergence of the numerical scheme is also seen by obtaining solution of this problem for various grid sizes.

The numerical scheme has been applied to obtain the variation of base shear force and base moment with time (Figure 9) of a cantilever Timoshenko Beam with material property such that the flexural and shear waves have same velocity ($kG = 1$) and subjected to unit linear velocity ($\bar{v}$) at the base. The numerical results are in good agreement with that obtained by Leonard and Budiansky |1| by Laplace transform technique. Error for the twenty-one grid sizes is not more than one unit. This problem has been given in detail in Appendix II.

Subsequently, a tapered cantilever beam ($\phi = 1^{o}$) has been subjected to a step input for diffirent durations

of time of the ground acceleration. The corresponding variation of base shear force and base moment with time are evaluated with the help of the numerical technique developed in Chapter III (Figure 10 and 11). Peaks of the response with time show diff-rences for various grid sizes for the input of short duration but the general trend of the curves are quite similar. On the other hand, when the duration of ground acceleration is large, a little deviation in the shear-time curve is observed at network of twenty-one grids from the shear-time curves of finer networks (41 and 81 grids). The moment-time curves are same for all practical purposes (difference in fourth significant figure).

In any numerical analysis the accuracy of the solution is limited by truncation and round off errors. Furthermore, a meaningful solution will be obtained if and only if the solution converges as the grid size is reduced. In the case of small duration of excitation the disparity in peak values for various grid-sizes may be due to the fact that the response created on the structure by the ground acceleration is appreciably small. Since the step by step integration uses the previous stage values of the variables to predict the same at an interval of time, there is possibility of error accumulation when the previous stage results are not quite accurate. Moreover, for coarser grid sizes the

possibility of incurring large error cannot be ignored and this explains the flattened response. However, when the duration of exitation is large the solutions show reasonable convergence for diffirent grid sizes (Figure 11). Similarity of results obtained by Leonard and Budiansky |1| and that obtained by numerical approach establishes perhaps conclusively the stability and convergence criteria of the solution as well as accuracy of the same.

4.2 DISCUSSION AND CONCLUSION

Firstly, change in the response of cantilever beams, with varying cross-section, subjected to ground acceleration has been studied. The material of the beam is assumed to be linearly elastic with no damping. The reduction of base shear force and base moment occur as the angle of taper (ϕ) increases (Figure 12). This follows directly from the elementary theory because reduction of the mass of the beam must give less moment and less shear at the base.

Secondly, effect of damping has been considered for a cantilever beam of linearly elastic material. The variation of base shear force and base moment with time has been plotted in Figure 13 and 14. The curves show that the damping ratio has a predominant effect on the response of structure as the time interval increases. The wave length of the response also increases with increase of the damping

ratio. This is in good agreement with the theory ($\omega_d = \sqrt{1-\mu^2}\,\omega_n$). A reduction of two third in the peak values of the bending moment and shear force at base are obtained between the cases when the damping ratio is zero and when it is 0.1. In this analysis the absolute damping is assumed proportional to fundamental model frequency due to inherent limitation of knowledge on the absolute damping of the material. This may lead to a prediction of higher responses from actual in the transient state of solution. However any firm conclusion on the prediction of actual response cannot be given unless the absolute damping of material is known with reasonable accuracy.

The method is finally employed to predict the transient stresses developed in the highest monolith of the Koyna-Concrete-Dam during the earthquake of 11th December, 1967. The material of the dam has been assumed linearly elastic with two diffirent viscous damping ratios ($\mu = 0.0035$ and $\mu = 0.1$). The absolute damping of the material has been evaluated using the fundamental frequency as given in an unpublished report with the help of numerical integration approach. The variation of bending stresses and shear force with time are plotted in Figure 15 to 38 at three different cross-section of the dam (A, B and C as shown in Figure 1). The following two cases are analysed in this study:

(a) The response of the dam having no water in the reservoir basin (Figure 15-26).

(b) The response of the dam with water in the reservoir basin (Figure 27-38).

In the former case (a) the maximum transient response reduces about fifty per cent as the damping ratio increases from μ = 0.0035 to μ = 0.1. The maximum transient response increases almost by sixty per cent in the latter case (b) from that of the former (a). In both the cases rapid changes in the values are indicated from the results.

When reservoir basin has no water and damping ratio of the material of the dam is 0.0035 the bending stresses exceed the allowable tensile limit at all cross-sections of the dam. These results have only theoretical importance of estimating the error that might occur in the response if the material of the dam is assumed to be linearly elastic without viscous damping. However, when the damping ratio is 0.1 the predicted maximum bending stresses exceeds the allowable limit only at section 'C' which conform to the cracking of the section at that level.

The maximum bending stresses are more than the allowable stresses in all the three cross-section of the dam for both values of damping ratio considering full water in

the reservoir basin. Th stress predicted are quite high owing to the limitation of Zanger's |7| theory. The concept of addition of virtual mass is liable to predict maximum stresses on the higher side than that of actual because the mass of water moving with the dam will not remain constant for the whole interval of time. Moreover no energy dissipation in the water is considered in this study.

In a strong earthquake the bendin stresses may be sufficiently large to exceed allowable stresses for a brief period of time. This does not imply failure of the structure since the stresses will be restrict d as soon as the ground motion and/or hydrodynamic force reverse or decrease.

However, it is felt that further study should be directed towards the generalisation of material properties for the dam. Since, concrete is neither elastic nor elasto-plastic and the stresses attain a very high value only for a short duration of time, investigation should be carried out considering the time dependent material properties and nonreversible factors such as redistribution of stresses due to cracking, energy dissipation due to damping etc. Again due to enormous bulk of a dam, the accurate prediction of material behaviour within it is quite impossible. Hence, probabilistic approach may be very suitable for this type of study.

Since two dimensional behaviour of dam subjected to ground acceleration and interaction between vibrating dam and the impounding water as a composite system, has not been thoroughly explored, investigations may also be directed towards these lines.

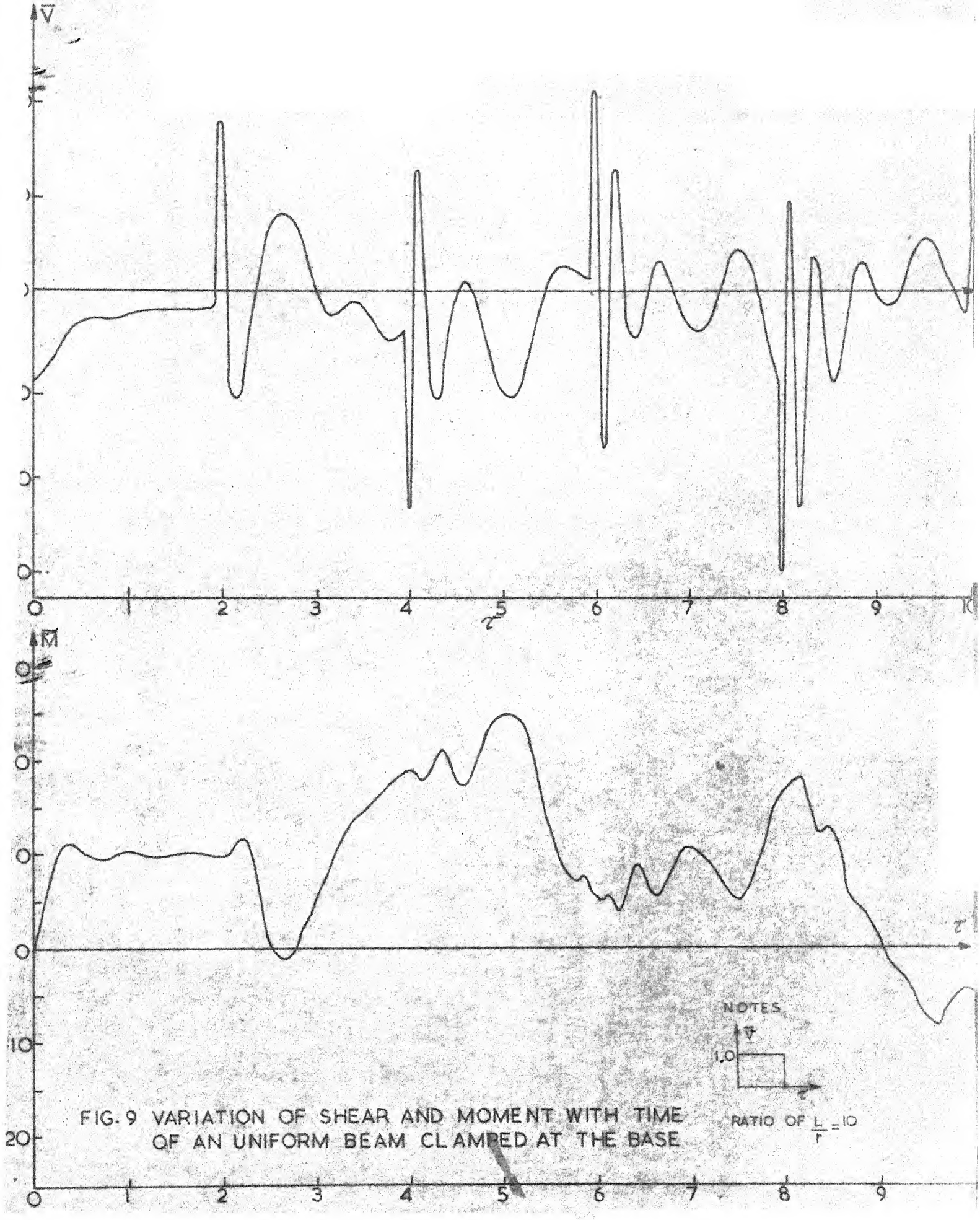

FIG. 9 VARIATION OF SHEAR AND MOMENT WITH TIME OF AN UNIFORM BEAM CLAMPED AT THE BASE

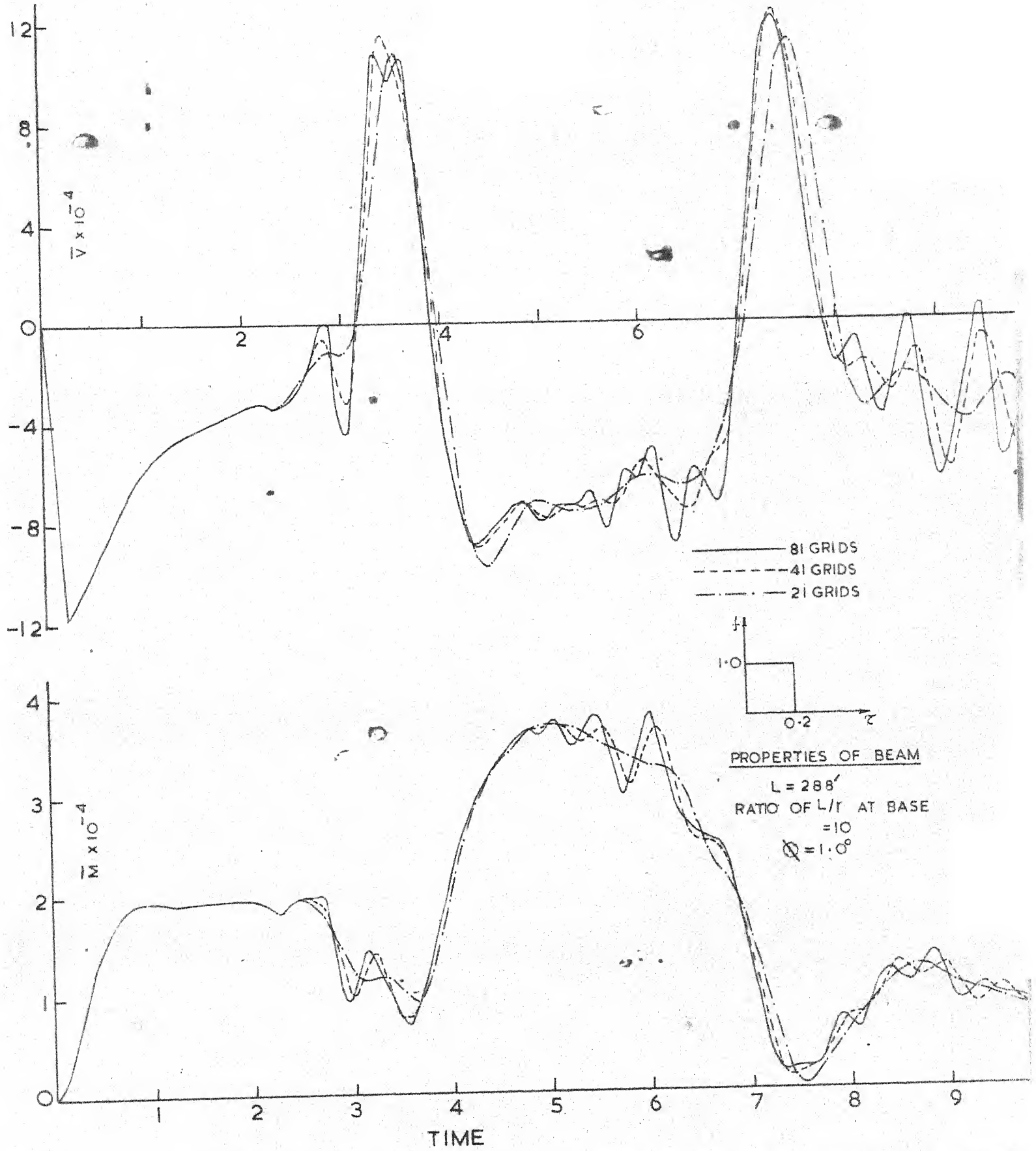

FIG. 10 CONVERGENCE OF NUMERICAL INTEGRATION WITH DIFFERENT GRIDS.

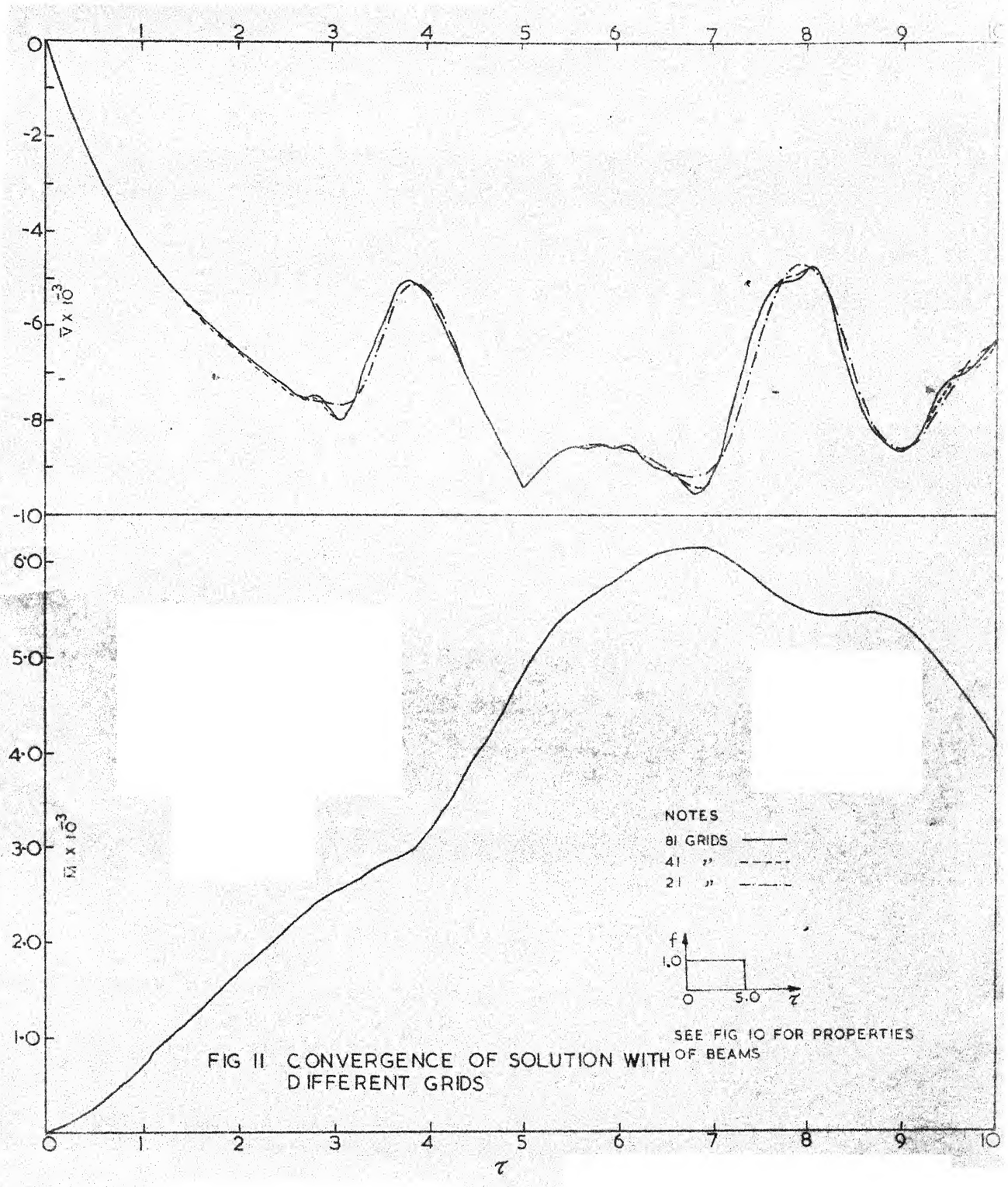

FIG 11 CONVERGENCE OF SOLUTION WITH DIFFERENT GRIDS

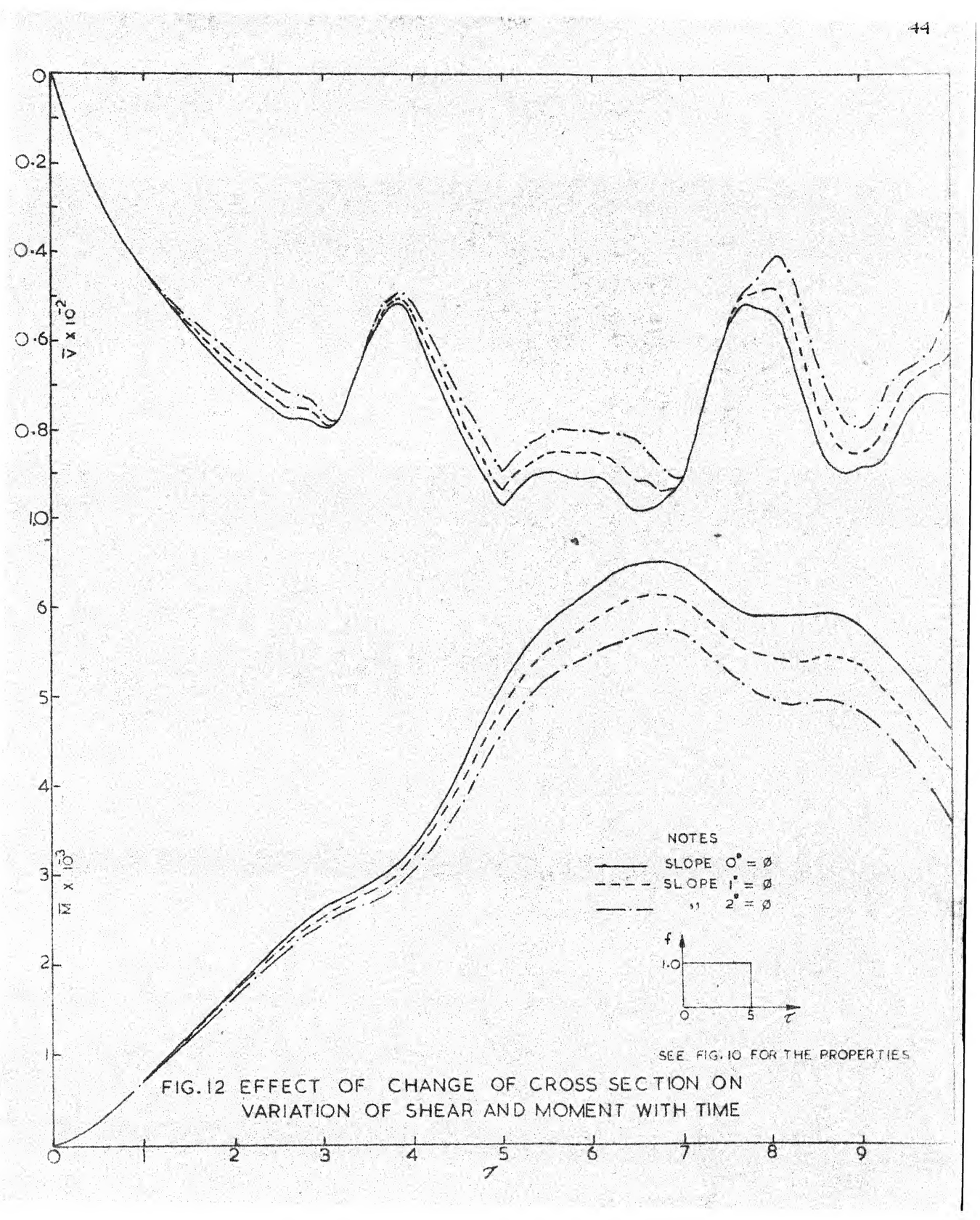

SEE FIG. 10 FOR THE PROPERTIES

FIG. 12 EFFECT OF CHANGE OF CROSS SECTION ON VARIATION OF SHEAR AND MOMENT WITH TIME

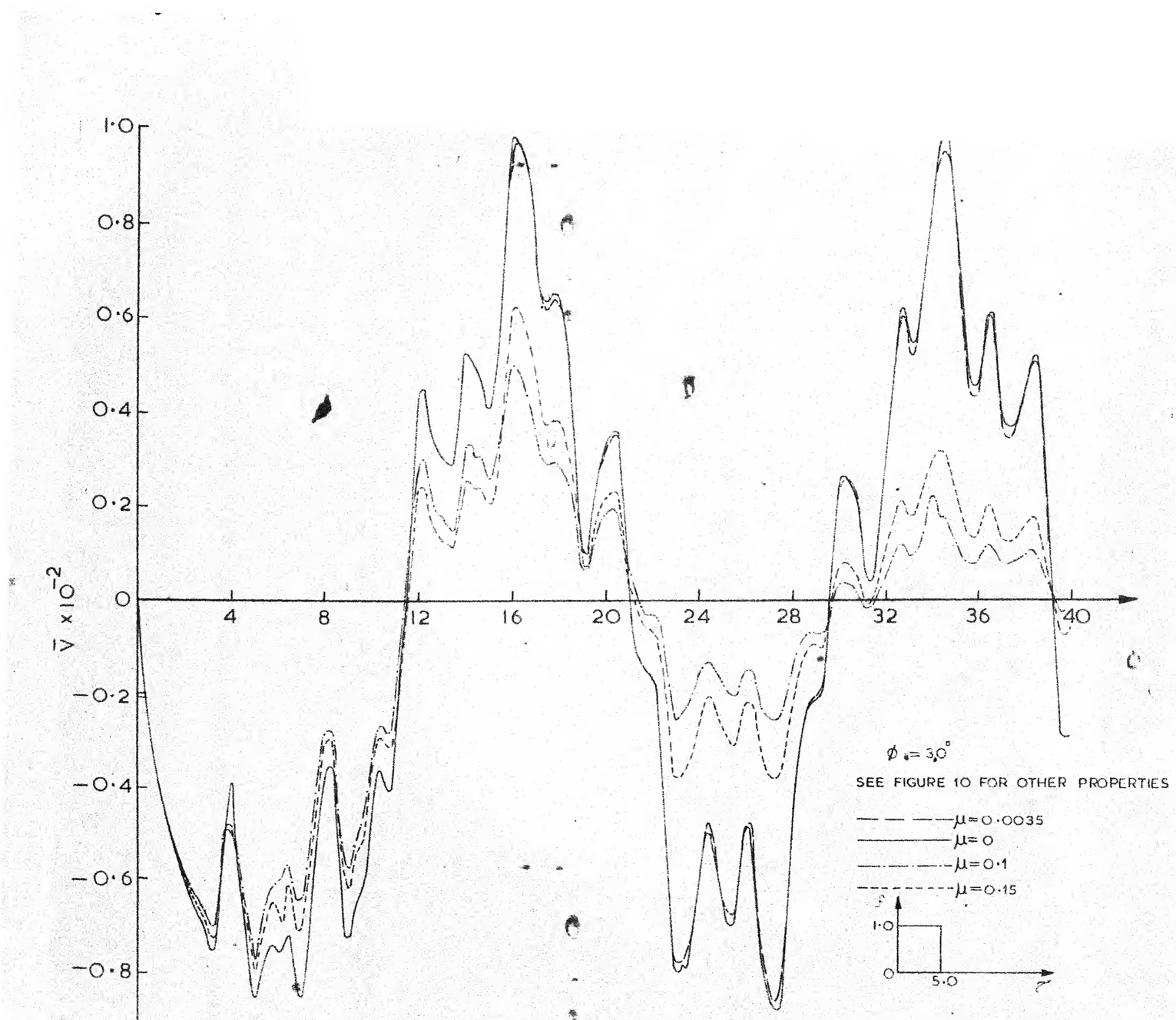

FIG. 13 VARIATION OF SHEAR WITH TIME FOR DIFFERENT DAMPING.

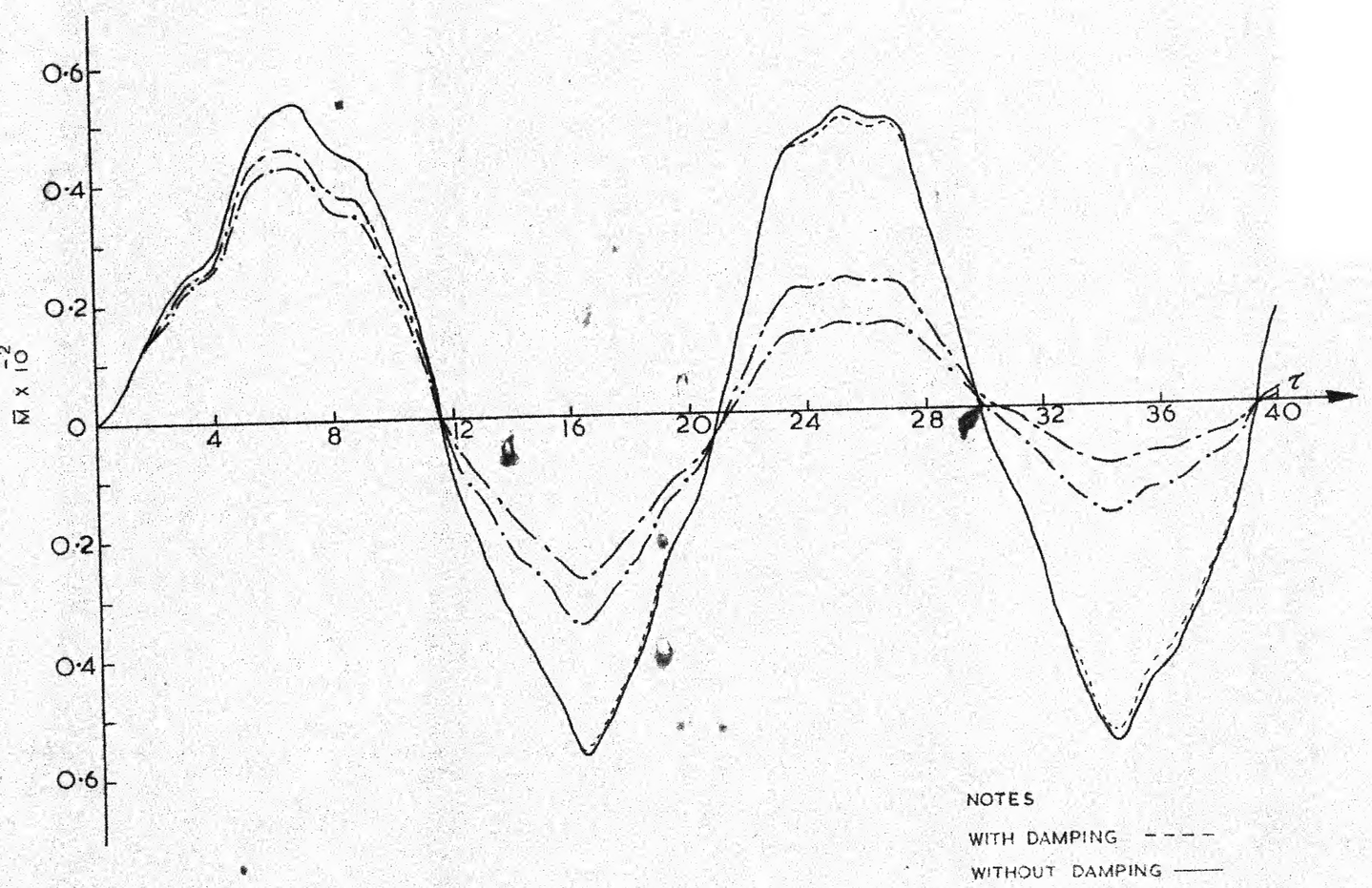

NOTES

WITH DAMPING - - - -

WITHOUT DAMPING ——

WITH DAMPING (μ=0·1) ——·——

" " (μ=0·15) ——··——

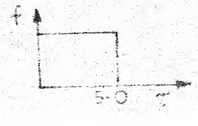

FIG. 14 VARIATION OF MOMENT WITH TIME FOR DIFFERENT DAMPING

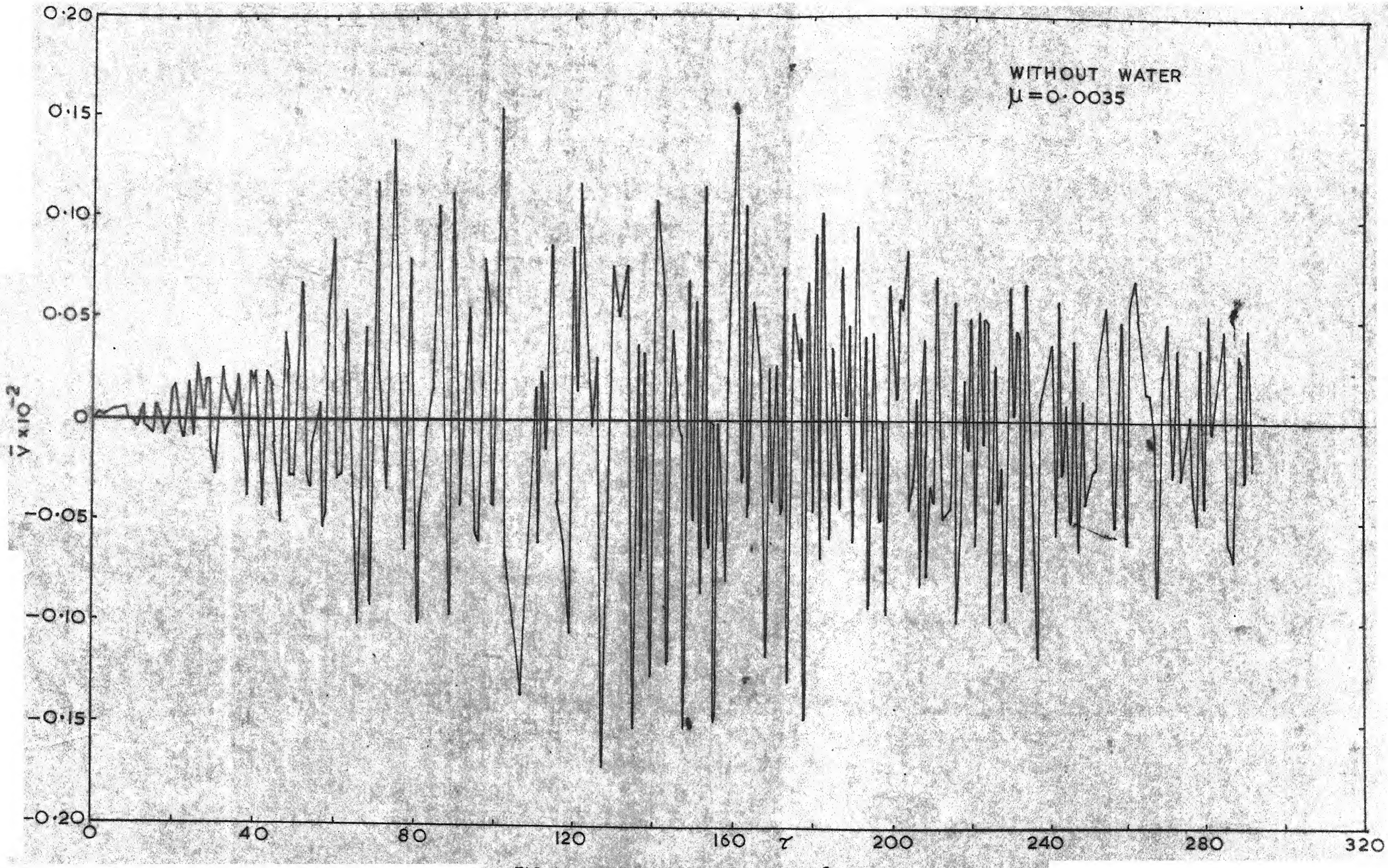

FIG.15 SHEAR FORCE - TIME (SECTION A)

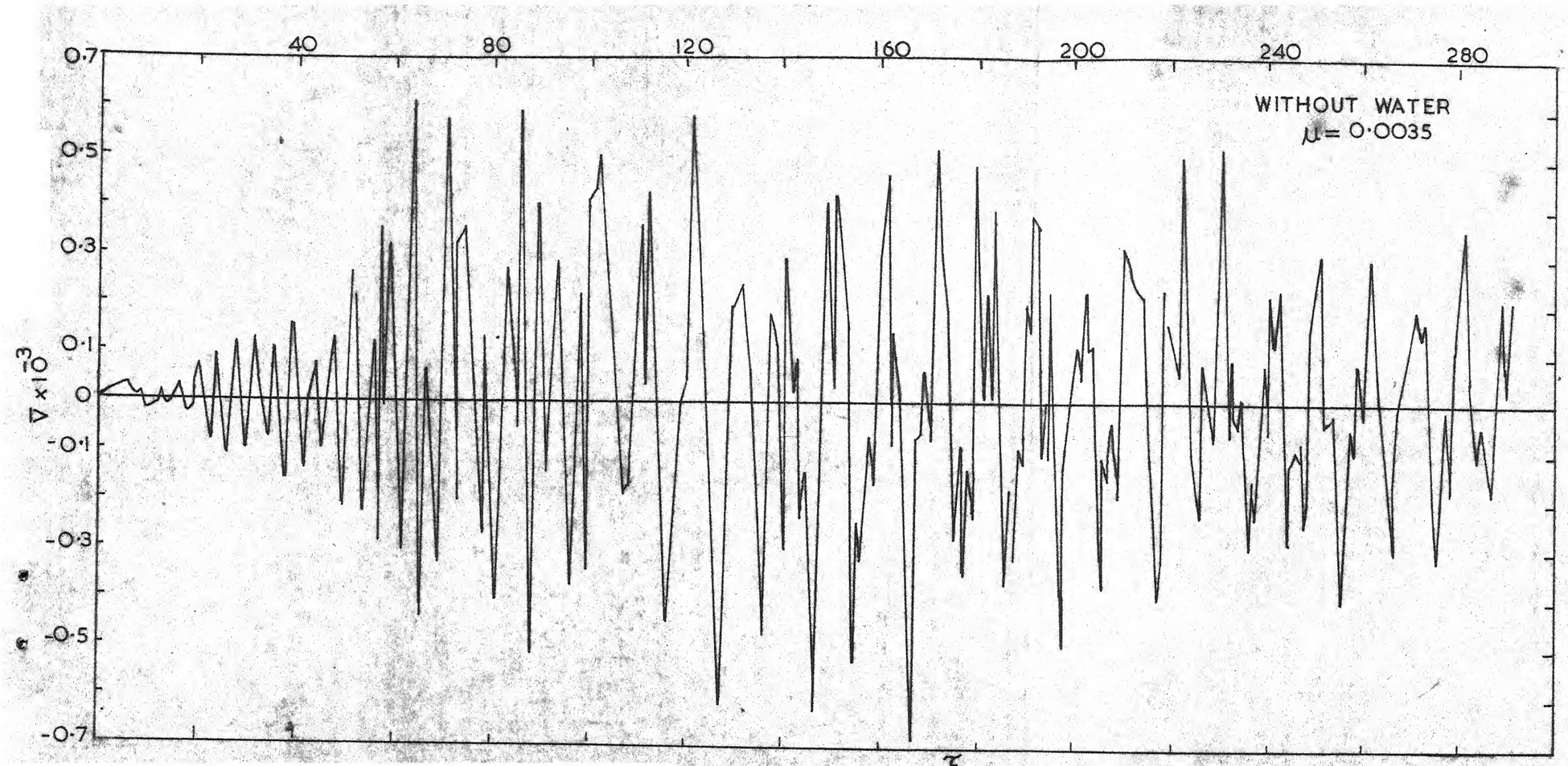

FIG. 16. SHEAR FORCE-TIME (SECTION B)

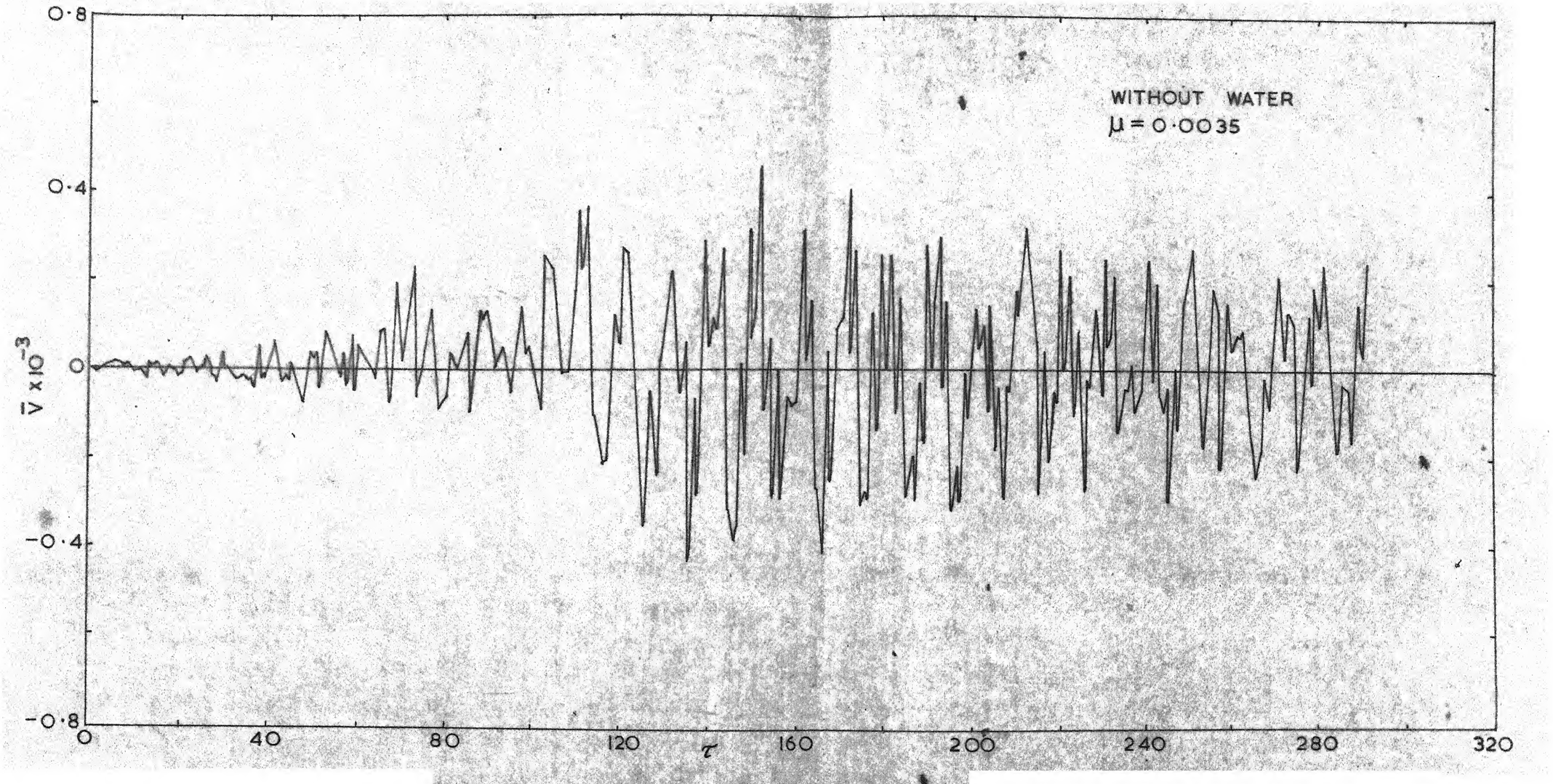

FIG·17 SHEAR FORCE – TIME (SECTION C)

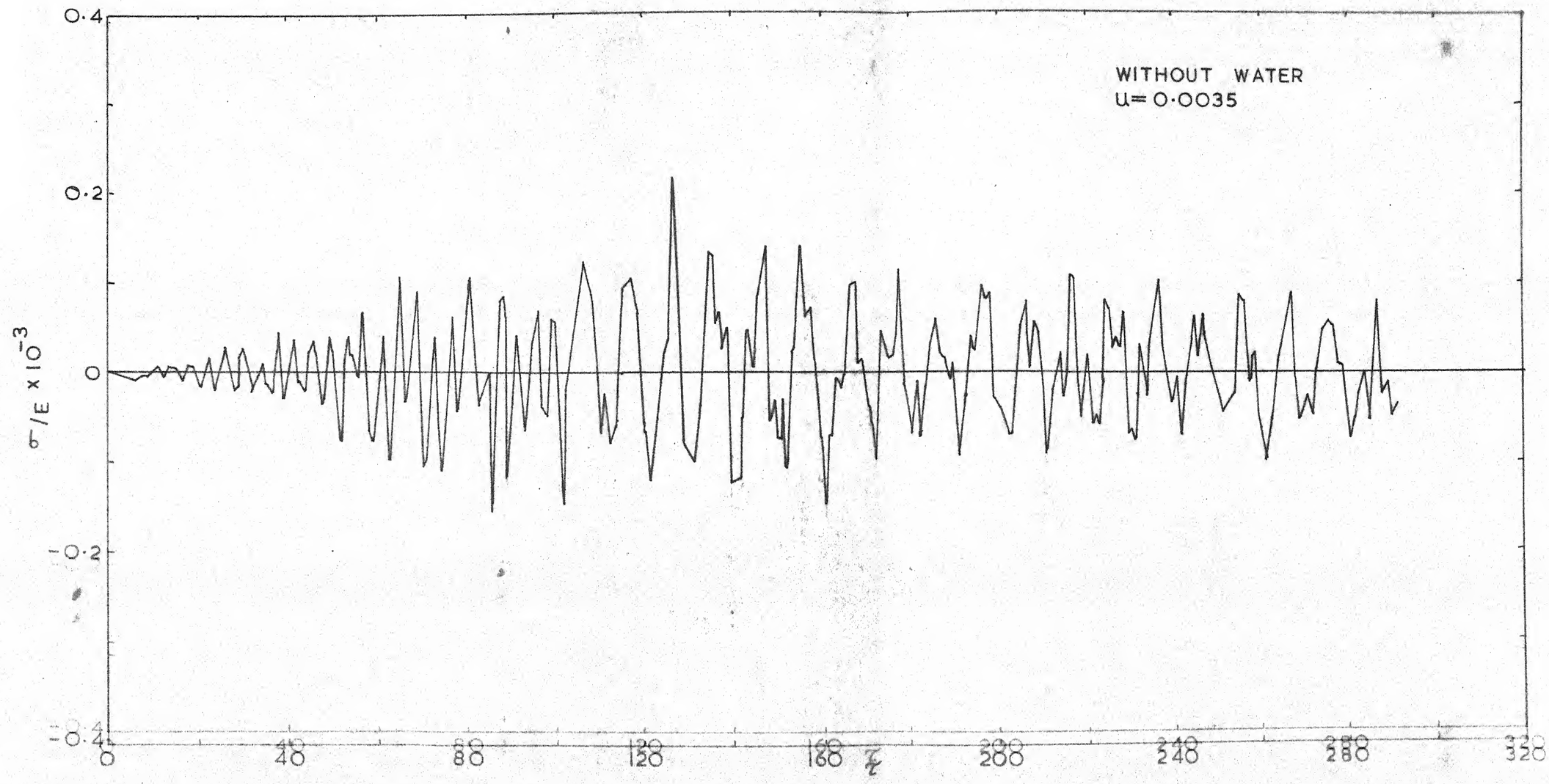

FIG. 18 BENDING STRESS- TIME (SECTION A)

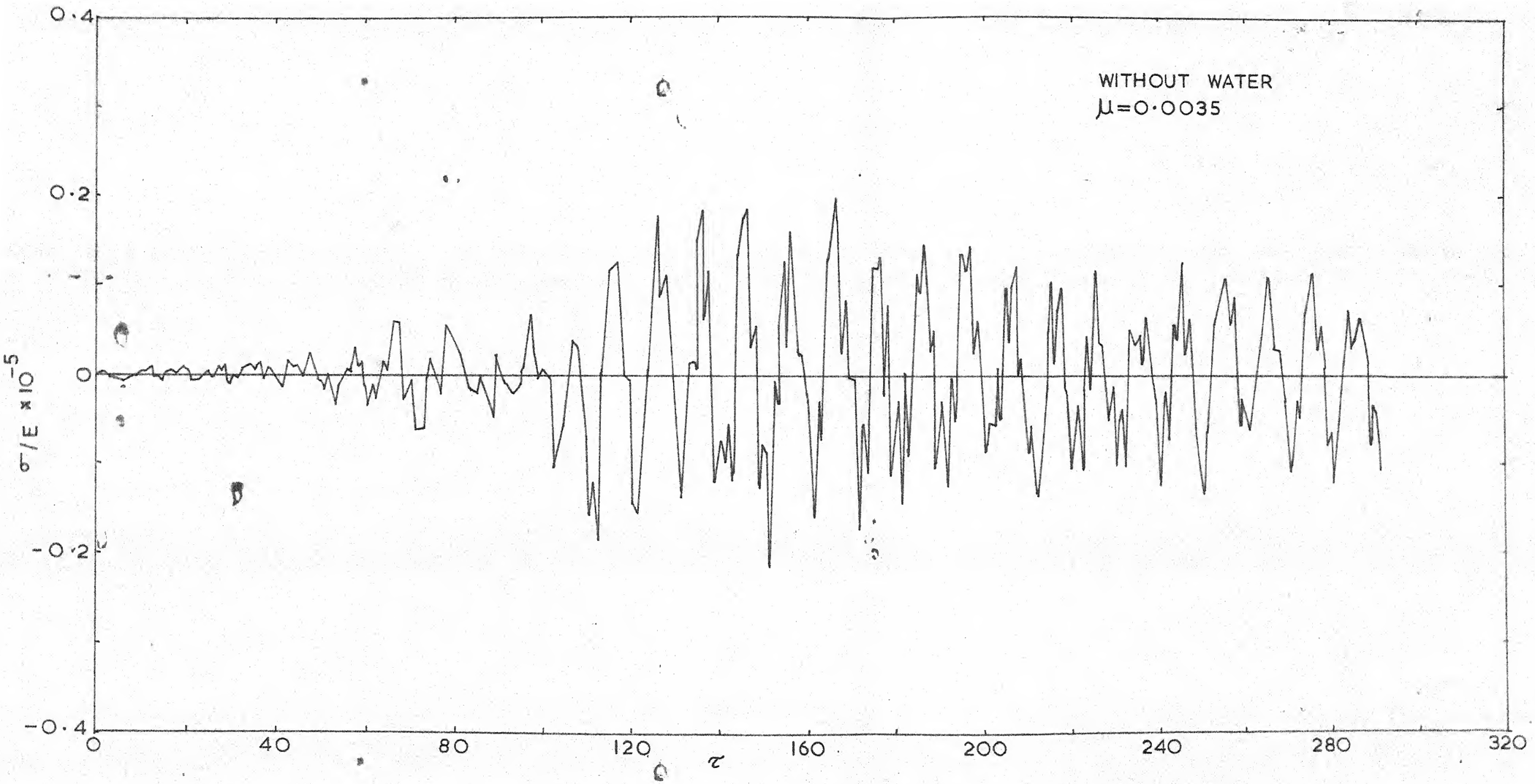

FIG.19 BENDING STRESS-TIME (SECTION B)

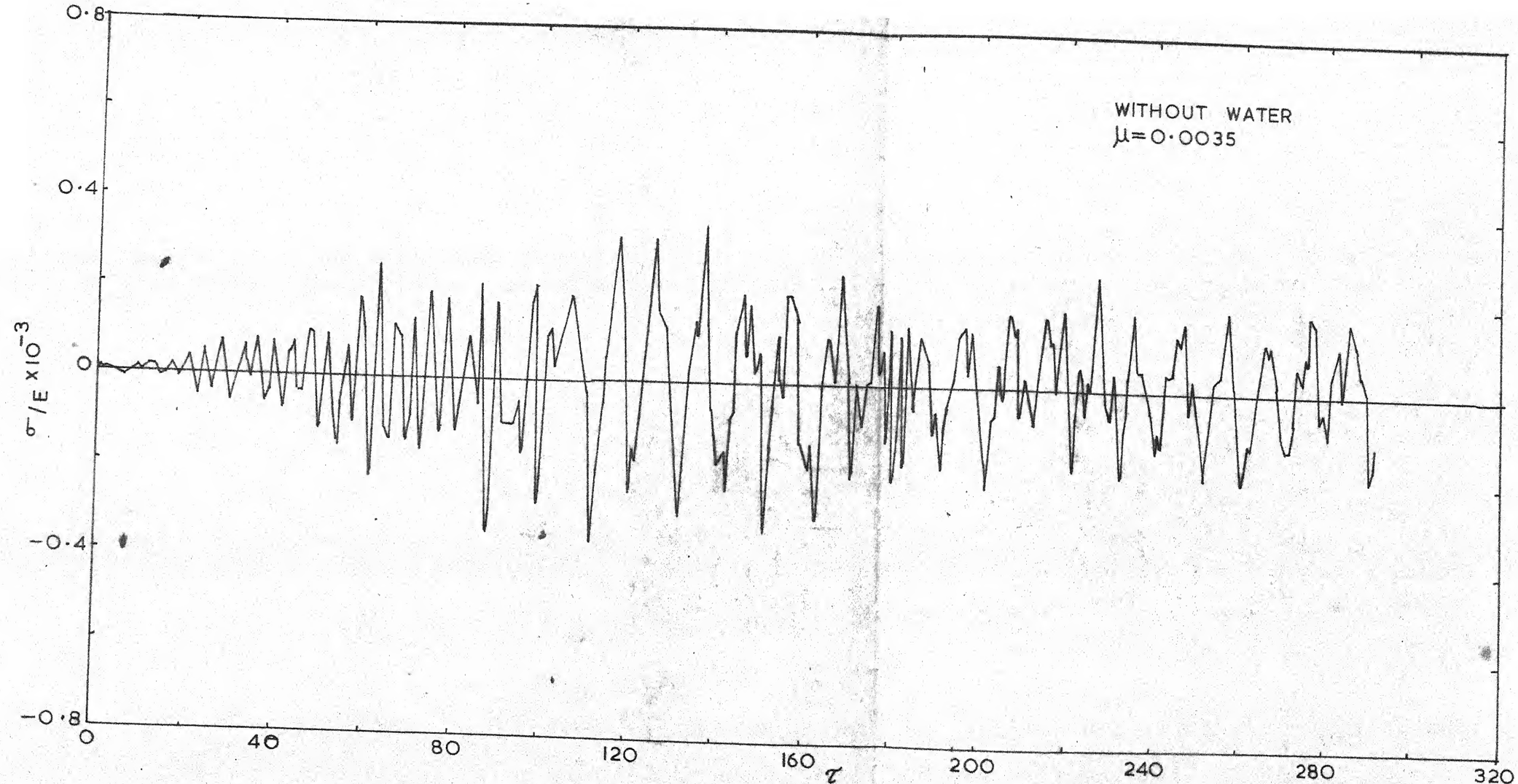

FIG·20 BENDING STRESS-TIME (SECTION C)

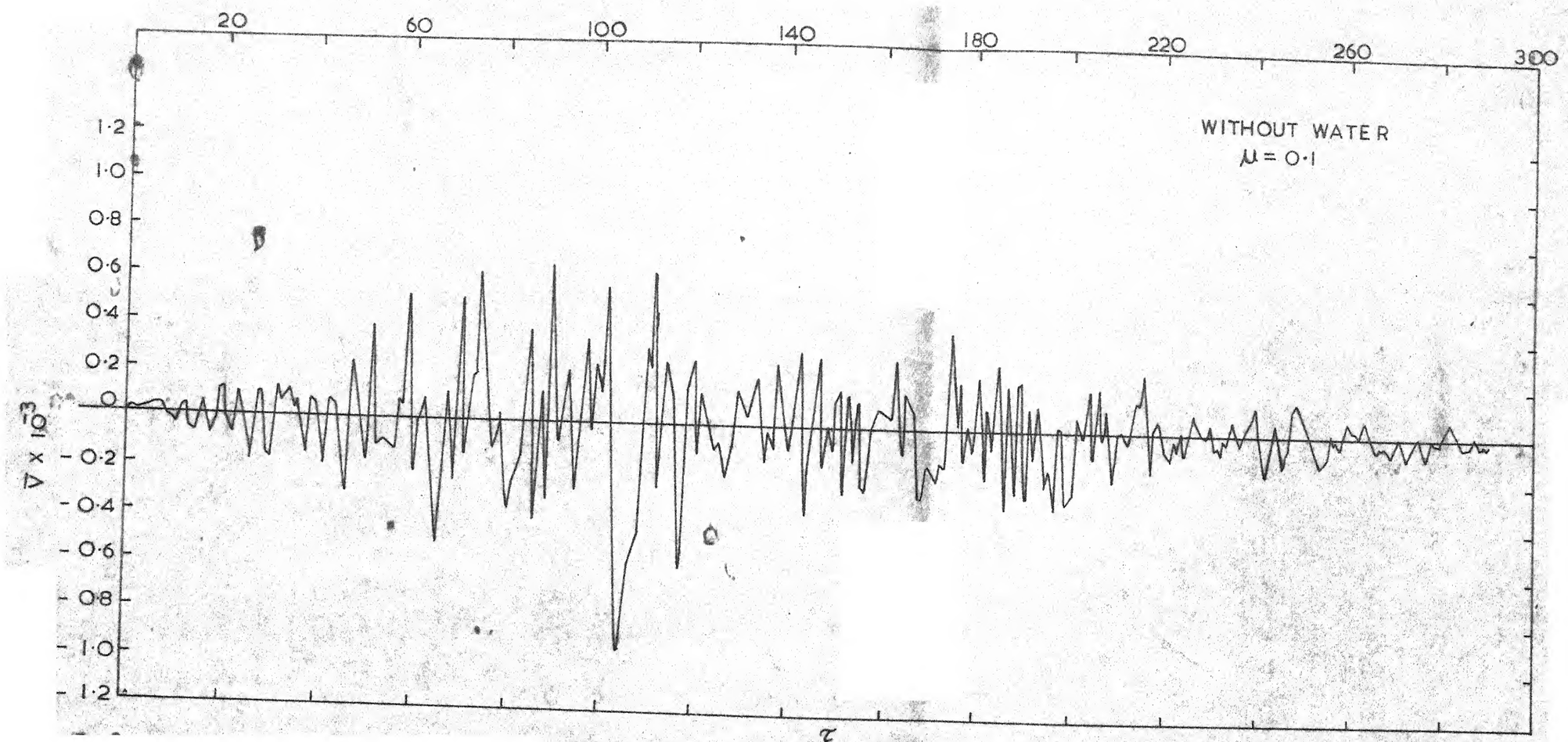

FIG. 21 SHEAR FORCE - TIME (SECTION A)

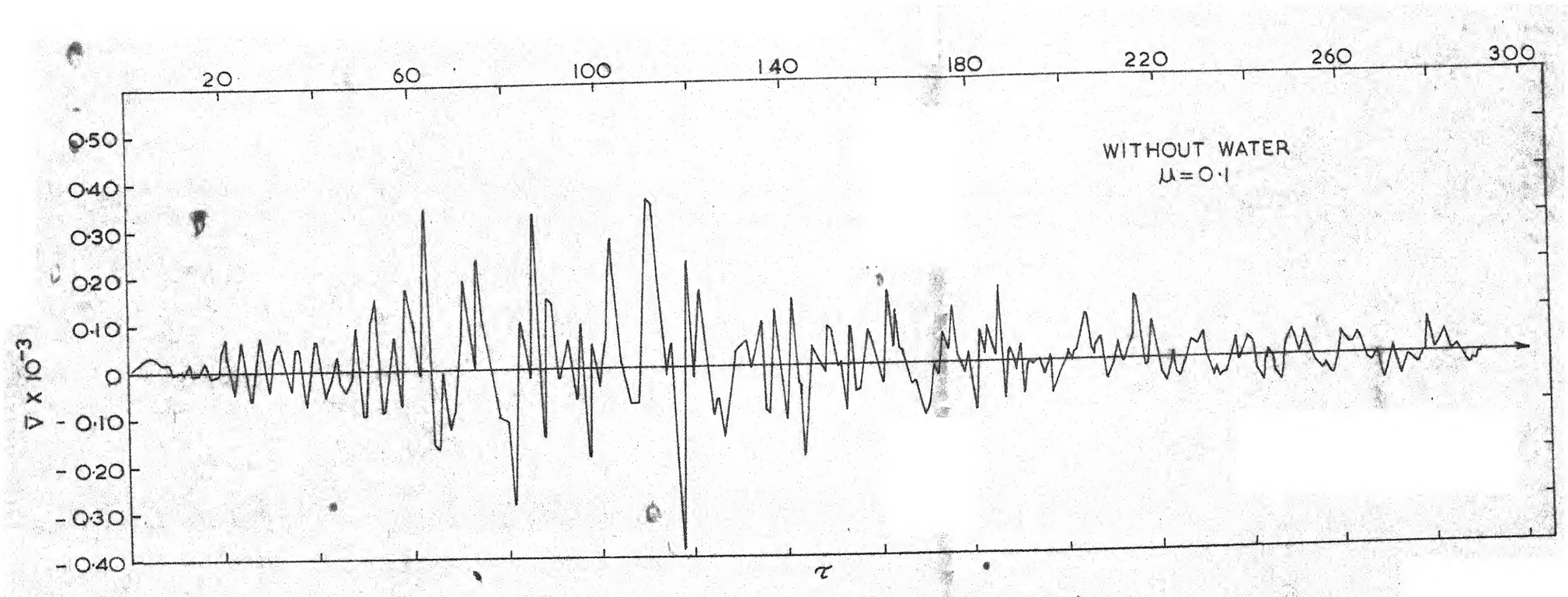

FIG.22. SHEAR FORCE TIME (SECTION B)

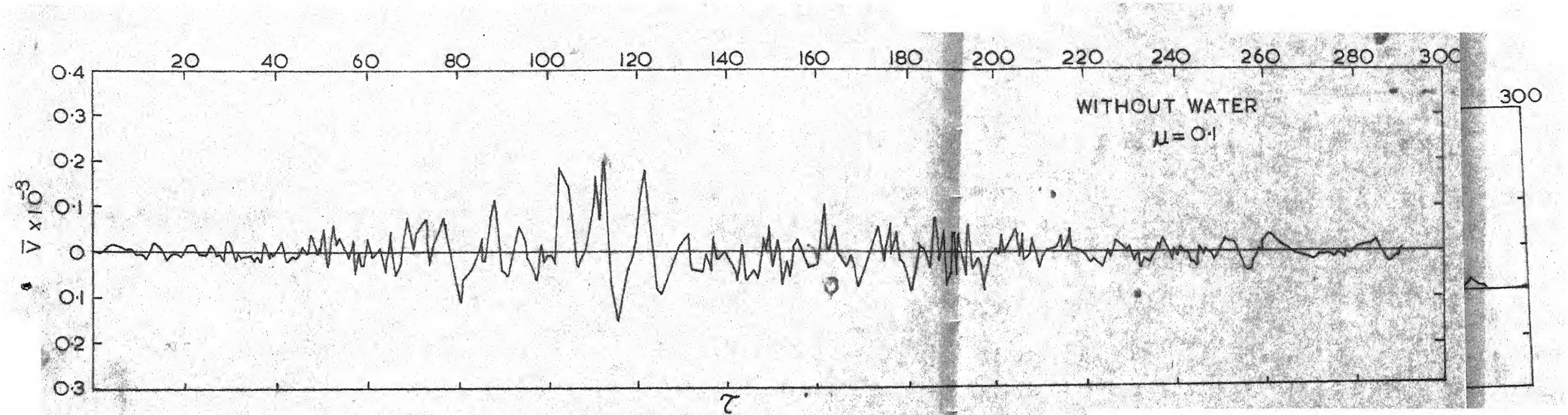

FIG 23 SHEAR FORCE-TIME (SECTION C)

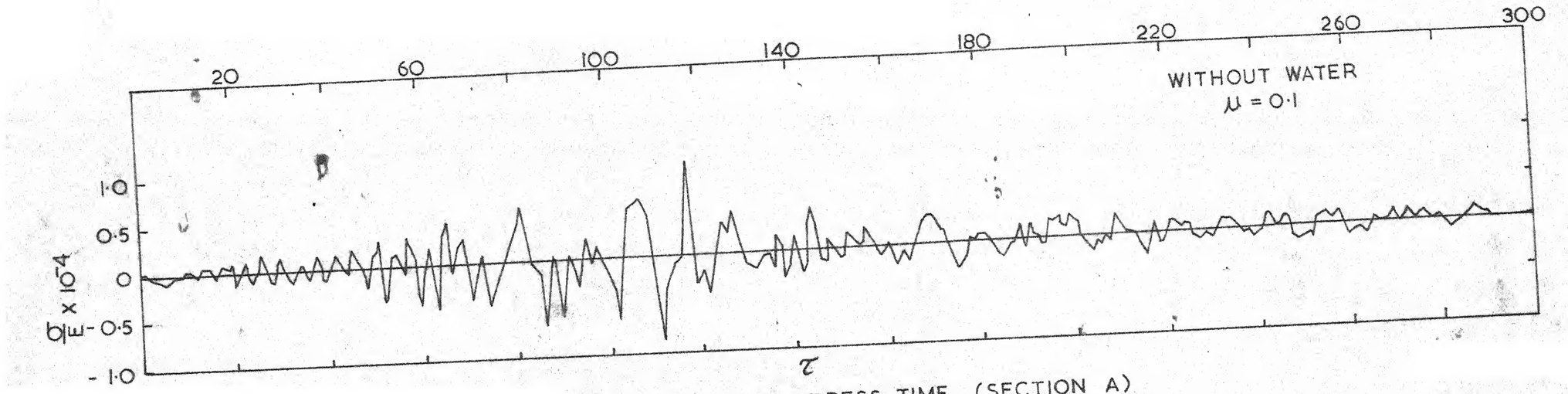

FIG.24. BENDING STRESS TIME (SECTION A)

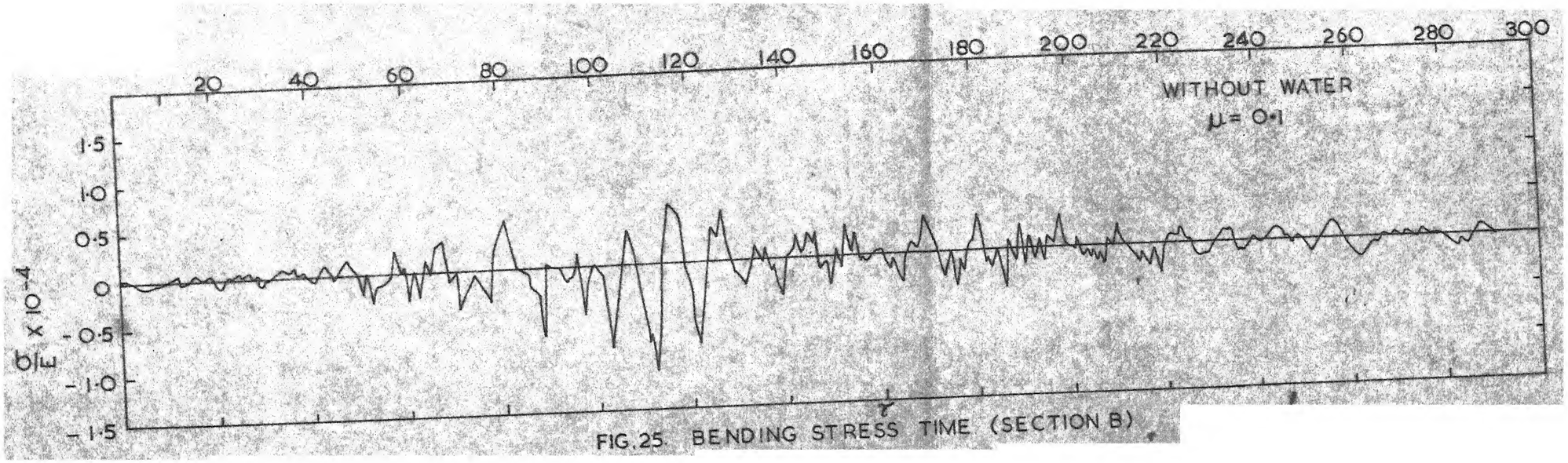

FIG. 25 BENDING STRESS TIME (SECTION B)

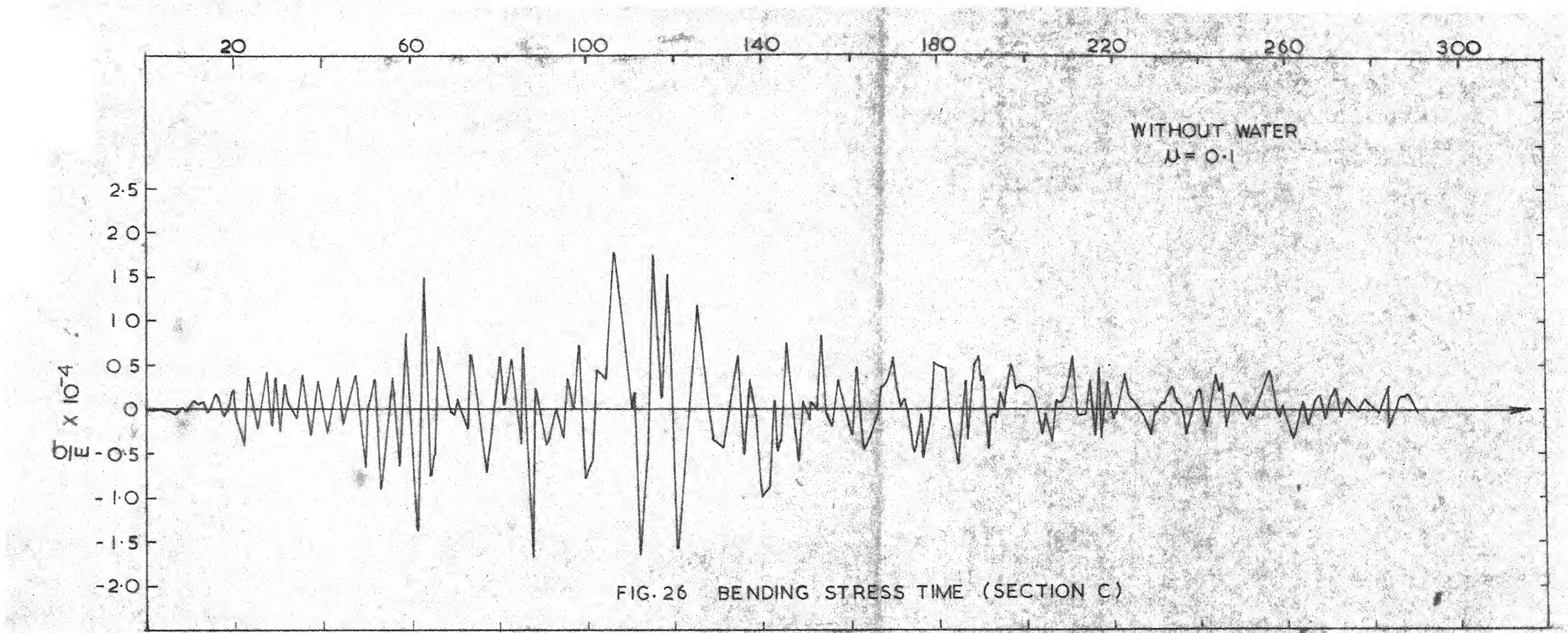

FIG. 26 BENDING STRESS TIME (SECTION C)

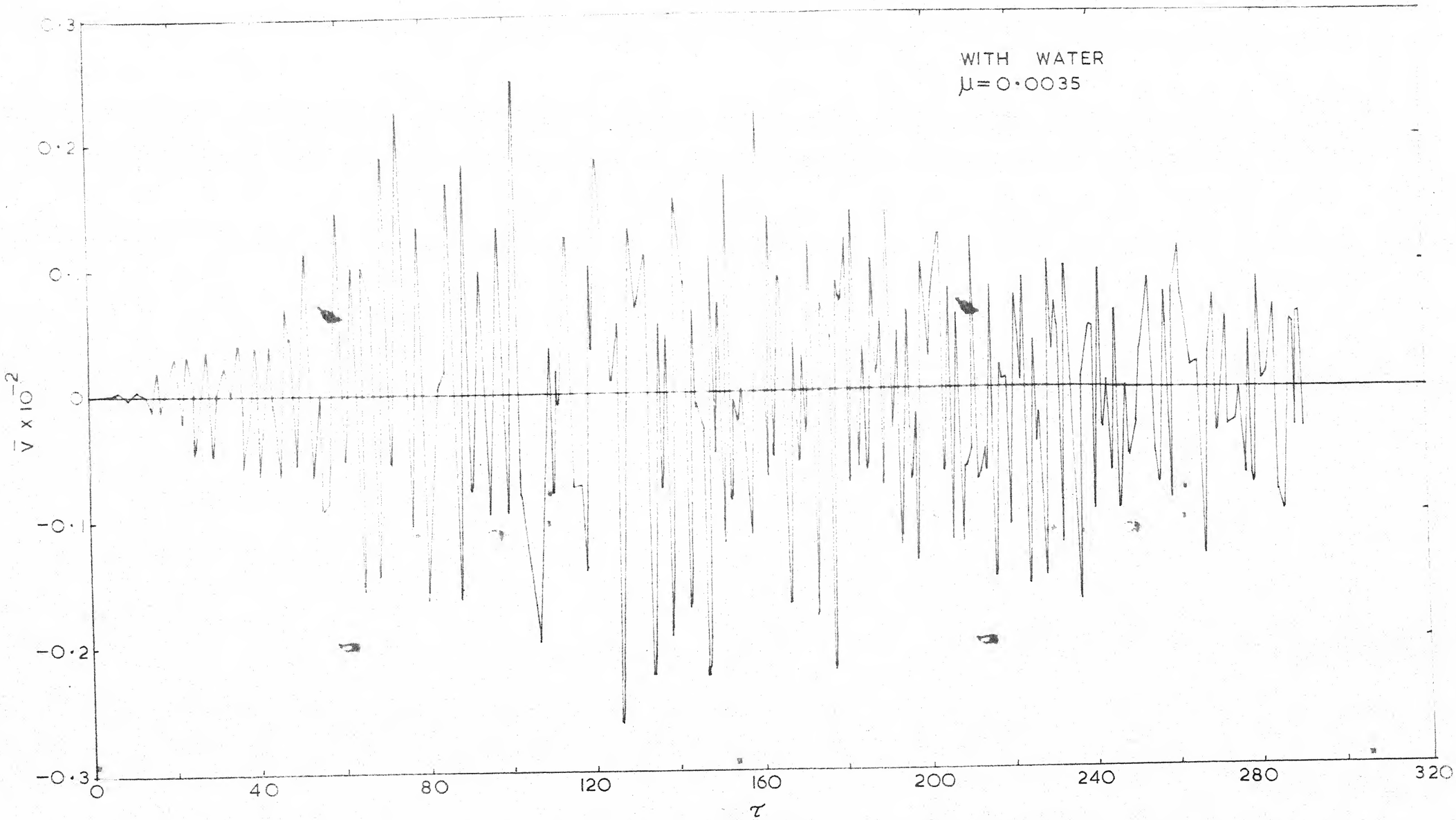

FIG·27 SHEAR FORCE – TIME (SECTION A)

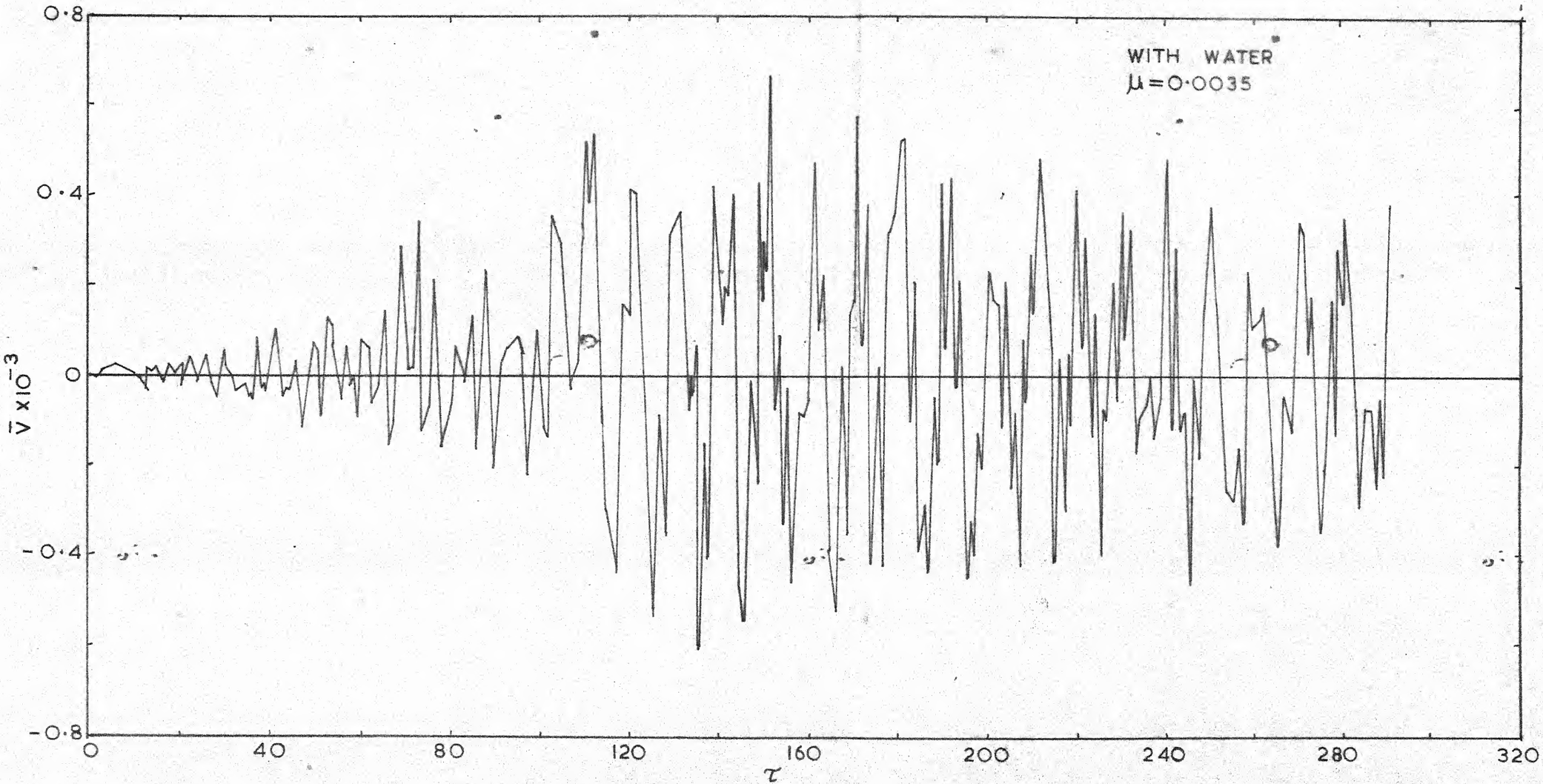

FIG·29 SHEAR FORCE - TIME (SECTION C)

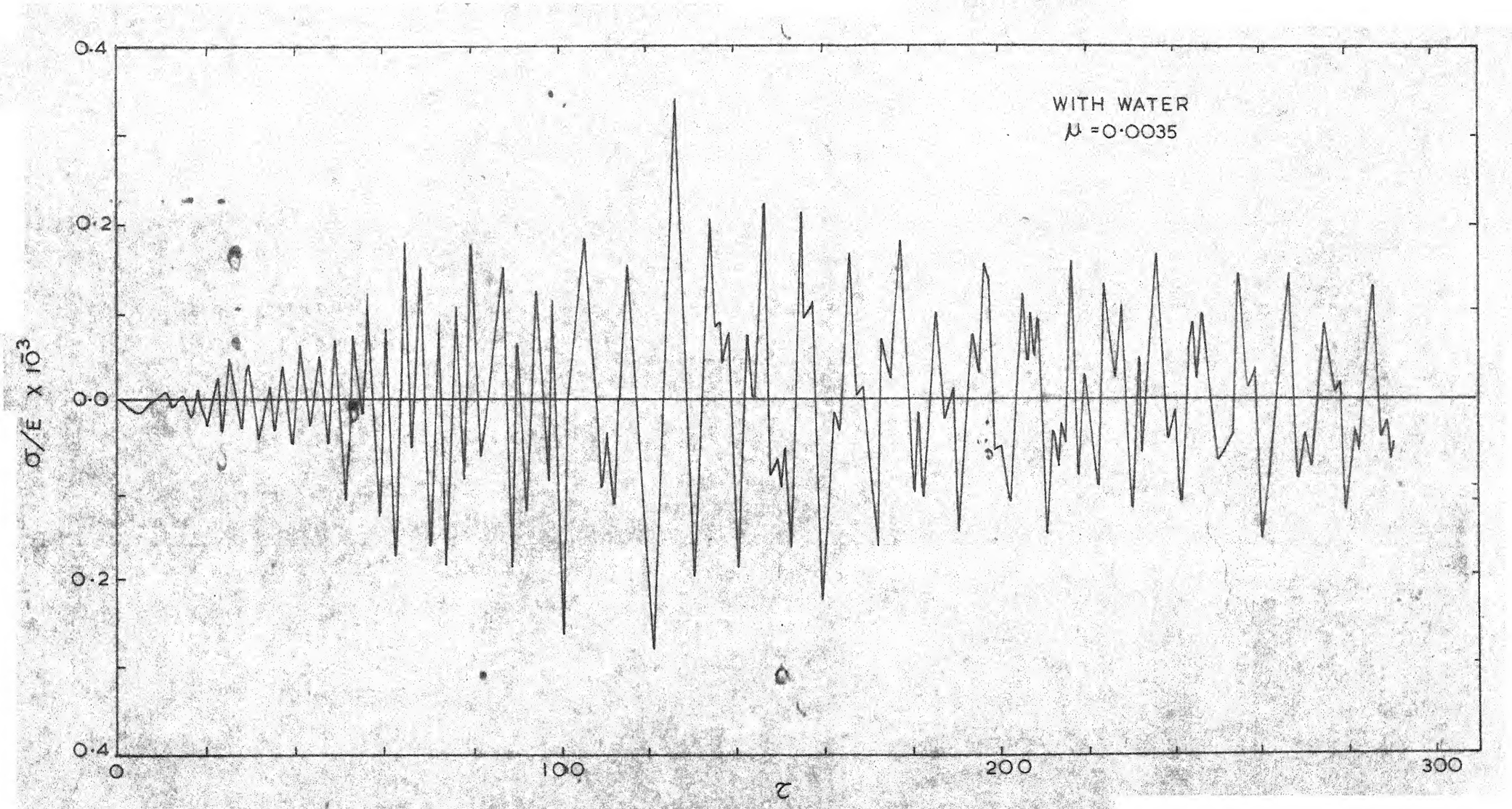

FIG. 30 BENDING STRESS-TIME (SECTION-A)

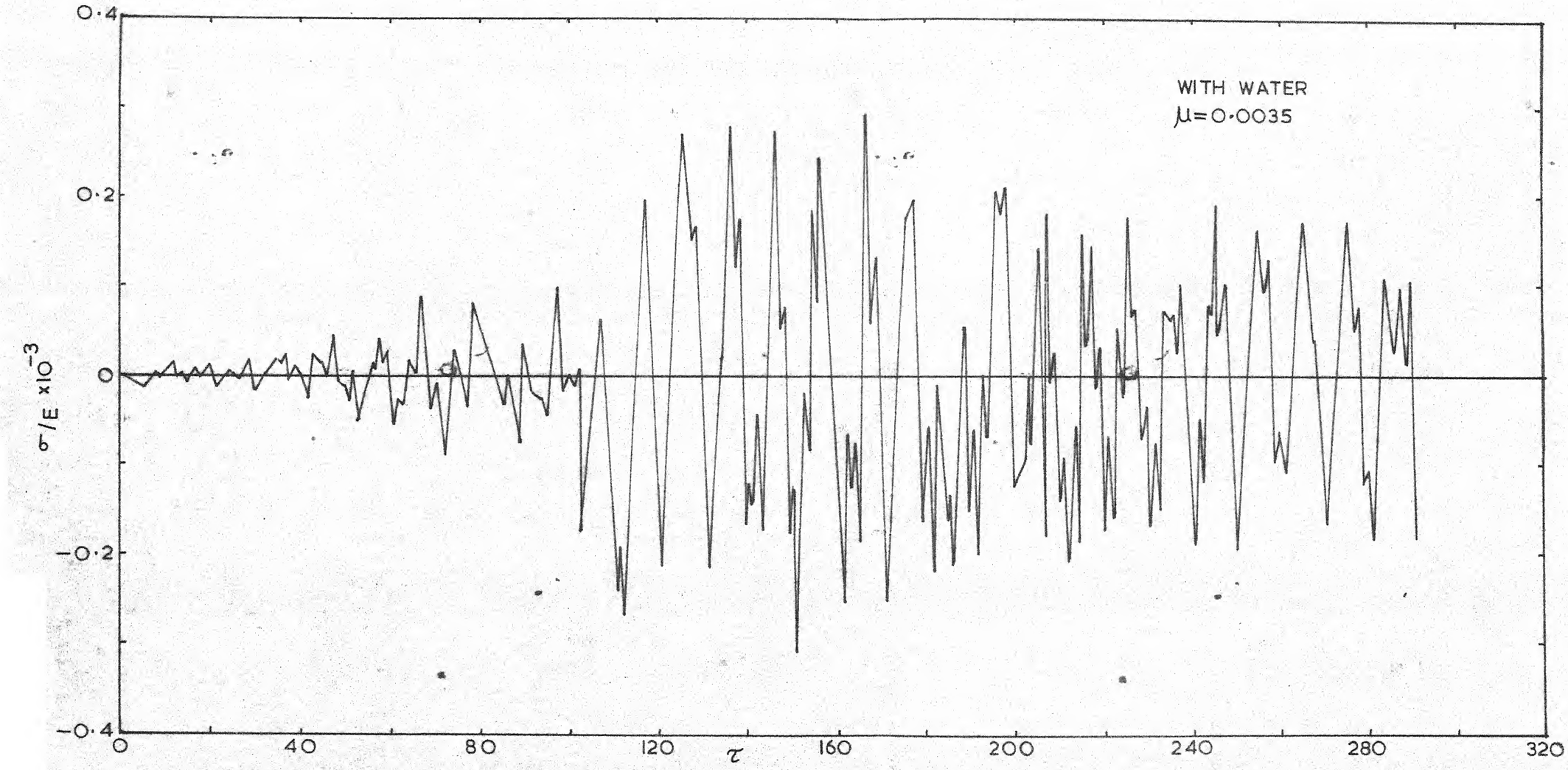

FIG. 31 BENDING STRESS–TIME (SECTION B)

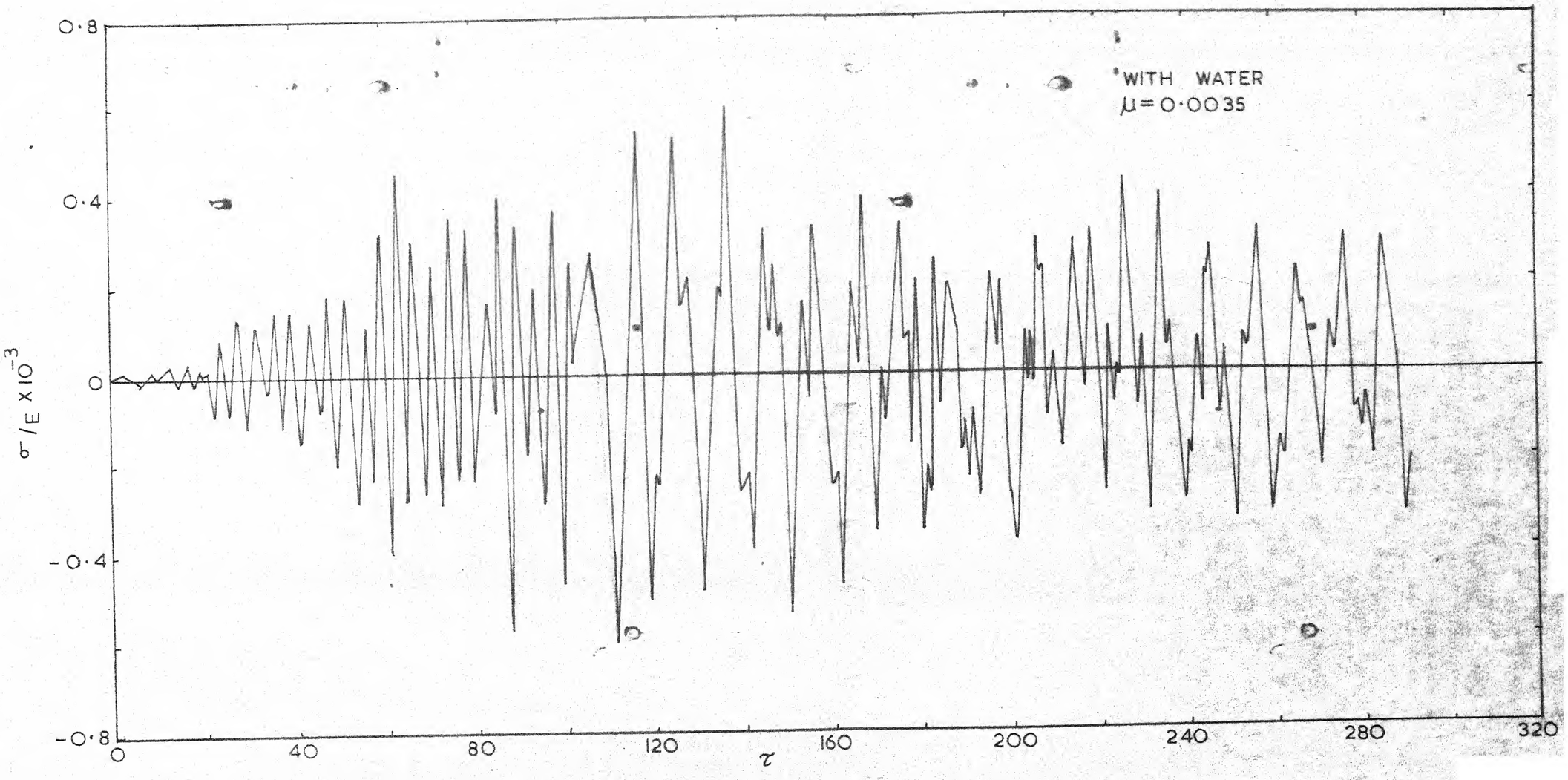

FIG. 32 BENDING STRESS – TIME (SECTION C)

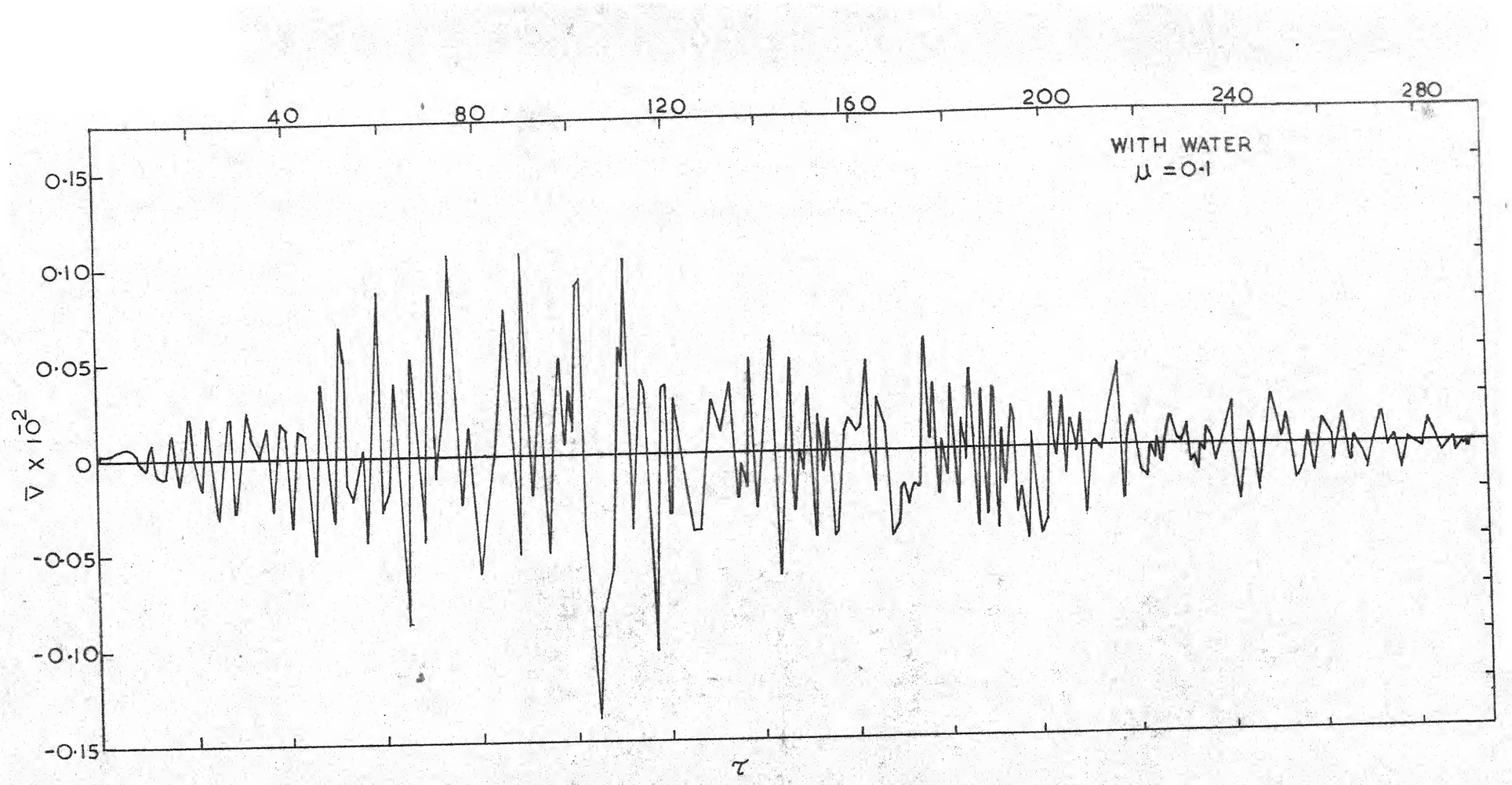

FIG.33 SHEAR FORCE-TIME (SECTION A)

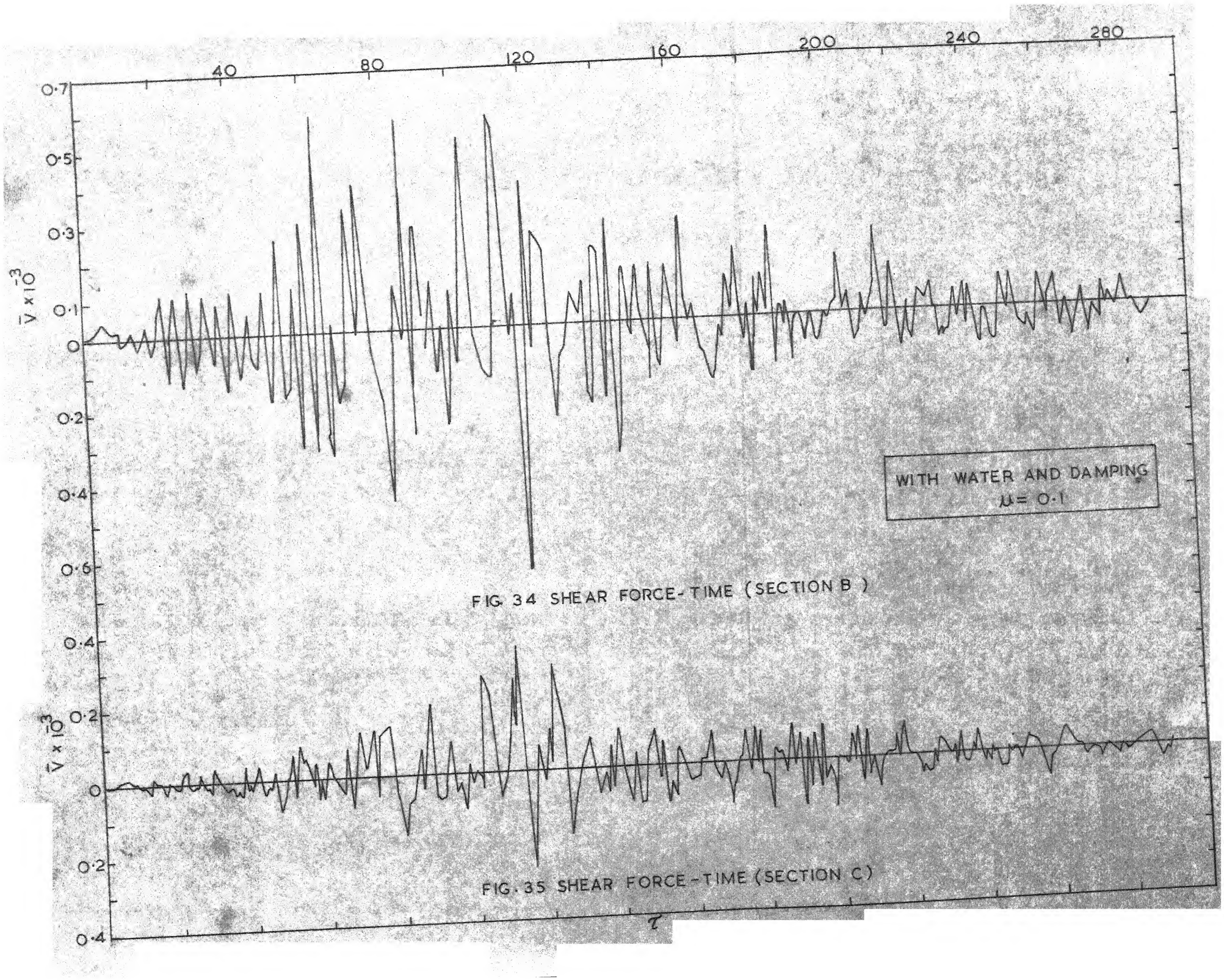

FIG. 34 SHEAR FORCE-TIME (SECTION B)

FIG. 35 SHEAR FORCE-TIME (SECTION C)

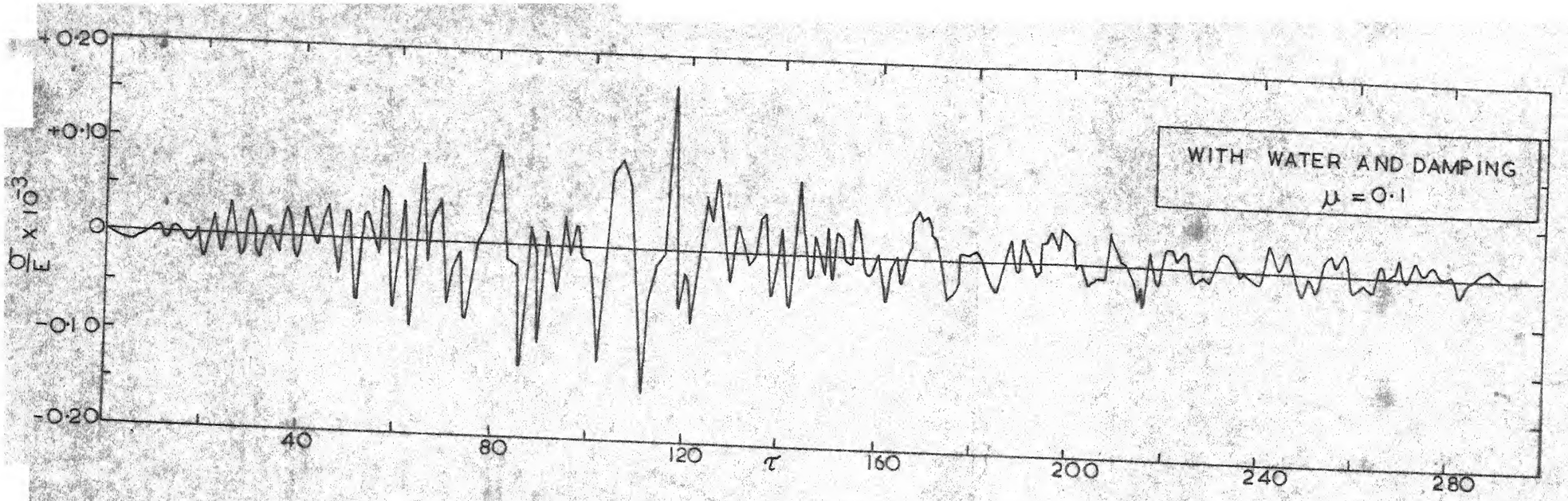

FIG. 36 BENDING STRESS-TIME (SECTION A)

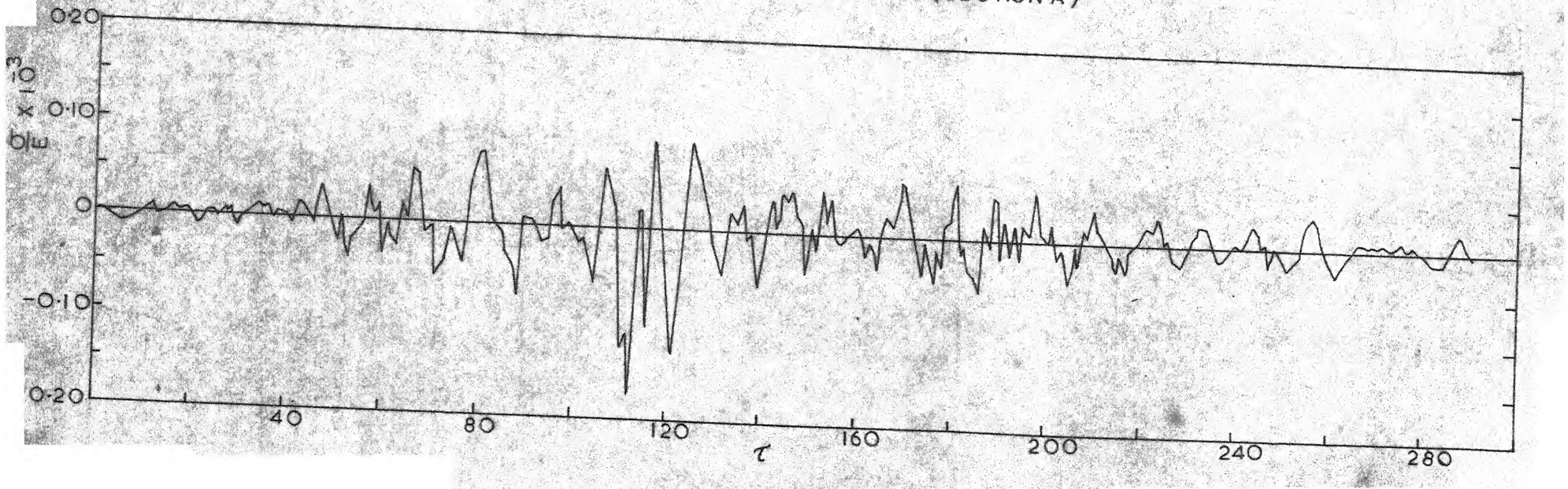

FIG. 37 BENDING STRESS-TIME (SECTION B)

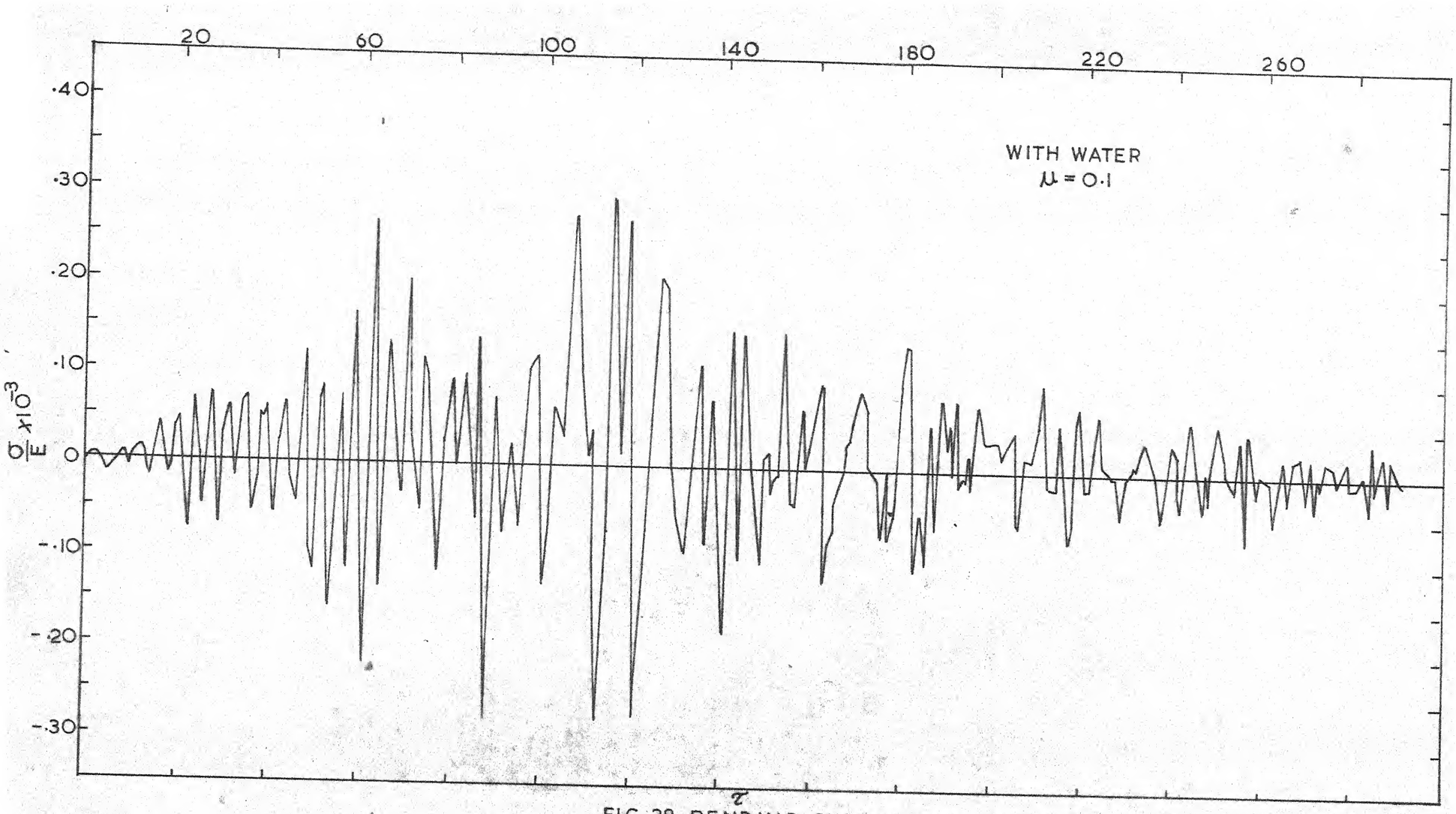

FIG. 38 BENDING STRESS-TIME (SECTION C)

APPENDIX - I

AI.1 DETAILS OF MATRICES, DETERMINANTS AND VECTORS USED IN ANALYSIS

The details of the matrices, determinants and vectors used in Chapter II and Chapter III are given in the followings:

$$[X] = \begin{bmatrix} d\tau & d\bar{x} & 0 & 0 & 0 & 0 & 0 & 0 \\ 0 & 0 & d\tau & d\bar{x} & 0 & 0 & 0 & 0 \\ 1 & 0 & 0 & \bar{I} & 0 & 0 & 0 & 0 \\ 0 & 1 & \bar{J} & 0 & 0 & 0 & 0 & 0 \\ 0 & 0 & 0 & 0 & d\tau & d\bar{x} & 0 & 0 \\ 0 & 0 & 0 & 0 & 0 & 0 & d\tau & d\bar{x} \\ 0 & 0 & 0 & 0 & \frac{1}{\xi A} & 0 & 0 & -1 \\ 0 & 0 & 0 & 0 & 0 & \frac{1}{A} & -\lambda & 0 \end{bmatrix} \qquad (A1.1)$$

$$\{Z\}^T = \langle \bar{M}_\tau \ \bar{M}_{\bar{x}} \ \bar{a}_\tau \ \bar{a}_{\bar{x}} \ \bar{V}_\tau \ \bar{V}_{\bar{x}} \ \bar{v}_\tau \ \bar{v}_{\bar{x}} \rangle \qquad (A1.2)$$

where

$\{Z\}^T$ = Transpose of $\{Z\}$

$$\{W\}^T = \left\langle d\bar{n} \ \ d\bar{a} \ \ 0 \ \ \bar{V} \ \ d\bar{V} \ \ d\bar{v} \ \ -\frac{k_1}{k_2}\bar{a} \ \ (\beta\bar{v}+\eta\alpha_f) \right\rangle \qquad (A1.3)$$

$|X|$ = Determinant of $[X]$ (A1.4)

$$|X| = \begin{vmatrix} d\bar{\tau} & d\bar{x} & 0 & 0 & 0 & 0 & 0 & 0 \\ d\bar{\sigma} & 0 & d\tau & d\bar{x} & 0 & 0 & 0 & 0 \\ 0 & 0 & 0 & \bar{I} & 0 & 0 & 0 & 0 \\ \bar{V} & 1 & \bar{J} & 0 & 0 & 0 & 0 & 0 \\ d\bar{V} & 0 & 0 & 0 & d\tau & d\bar{\tau} & 0 & 0 \\ d\bar{v} & 0 & 0 & 0 & 0 & 0 & d\tau & d\bar{\tau} \\ -\frac{k_1}{k_2}\bar{a} & 0 & 0 & 0 & \frac{1}{\bar{A}} & 0 & 0 & -1 \\ \beta\bar{v}+\eta\alpha_f & 0 & 0 & 0 & 0 & \frac{1}{\bar{A}} & -\lambda & 0 \end{vmatrix}$$

(A1.5)

$$\{U\}^T = \langle \bar{V} \quad \bar{v} \quad \bar{a} \quad \bar{M} \rangle_{J,k} \qquad \text{(A1.6)}$$

$$[B] = \begin{bmatrix} \frac{d\tau}{2} & 0 & -\frac{1}{2}J_{1-2} & -C_1 \\ -\frac{2}{A_{1-1}} & \lambda'+\frac{\rho' d\tau}{2} & -\frac{\lambda' d\tau}{2} & 0 \\ -\frac{2}{A_{1+1}} & -(\lambda'+\frac{\rho' d\tau}{2}) & -\frac{\lambda' d\tau}{2} & 0 \\ \frac{d\tau}{2} & 0 & -\frac{1}{2}J_{1+2} & -C_1 \end{bmatrix}$$

(A1.7)

$$[B]^{-1} = \frac{1}{|B|}\begin{vmatrix} a_1 & a_2 & a_2 & a_1 \\ a_3 & a_4 & a_5 & a_3 \\ a_6 & a_7 & a_7 & a_6 \\ a_8 & a_9 & a_9 & a_{10} \end{vmatrix} \qquad (A1.3)$$

where

$$|B| = -C_1(\rho' \frac{d\tau}{2} + \lambda')(\frac{J_n}{A_{1-1}\, A_{1+1}} + \lambda' d\tau^2)$$

$$a_1 = -C_1 \lambda' d\tau \,(\rho' \frac{d\tau}{2} + \lambda')$$

$$a_2 = \frac{C_1 J}{2}(\rho' \frac{d\tau}{2} + \lambda')$$

$$a_3 = -C_1 \lambda' d\tau \,(A_{1+1} - A_{1-1})/(A_{1+1}\, A_{1-1})$$

$$a_4 = -C_1 (\lambda' d\tau^2/2 + J/A_{1+1})$$

$$a_5 = C_1(\lambda' d\tau^2/2 + J/A_{1-1})$$

$$a_6 = 2AC_1(\rho' d\tau/2 + \lambda')/(A_{1+1}\, A_{1-1})$$

$$a_7 = C_1 d\tau \,(\rho' \frac{d\tau}{2} + \lambda')$$

$$a_8 = (\rho' \frac{d\tau}{2} + \lambda')(\frac{A\, J_{1+1}}{A_{1+1}\, A_{1-1}} + \frac{\lambda' d\tau^2}{2})$$

$$a_9 = \frac{d\tau}{4}\left(\frac{\beta' d\tau}{2} + \lambda'\right)\left(J_{1+2} - J_{1-2}\right)$$

$$a_{10} = -\left(\beta' d\tau/2 + \lambda'\right)\left(\frac{AJ_{1-2}}{A_{1+1}\,A_{1-1}} + \frac{\lambda' d\tau^2}{2}\right)$$

$$A = A_{1+1} + A_{1-1}$$

$$J = J_{1+2} + J_{1-2}$$

$$[C] = [c_{mj}] \quad (m = 1,\ldots 4,\ j = 1,\ldots 12) \qquad (A1.3)$$

where

$$c_{1\,1} = c_{4\,10} = -d\tau/2$$

$$c_{1\,2} = -c_1$$

$$c_{1\,5} = -J_{1-2}/2$$

$$c_{2\,4} = -2/A_{1-1}$$

$$c_{2\,5} = \lambda' - \beta' d\tau/2$$

$$c_{2\,6} = c_{3\,9} = \lambda' d\tau/2$$

$$c_{3\,7} = -2/A_{1+1}$$

$$c_{3\,8} = \beta' d\tau/2 - \lambda'$$

$$c_{4\ 11} = c_1$$

$$c_{4\ 12} = -J_{i+2}/2$$

and all other $c_{mJ} = 0$

$$\{P\}^T = \langle \bar{V}_{i-2} \quad \bar{v}_{i-2} \quad \bar{a}_{i-2} \quad \bar{V}_{i-1} \quad \bar{v}_{i-1} \quad \bar{a}_{i-1}$$

$$\bar{V}_{i+1} \quad \bar{v}_{i+1} \quad \bar{a}_{i+1} \quad \bar{V}_{i+2} \quad \bar{M}_{i+2} \quad \bar{a}_{i+2} \rangle, k-1 \qquad (A1.10)$$

$$\{Q\} = \begin{Bmatrix} 0 \\ -F(\alpha_J + \alpha_{i-1})d\tau \\ F(\alpha_J + \alpha_{i+1})d\tau \\ 0 \end{Bmatrix} \qquad (A1.11)$$

$$[D]^{-1} = \begin{bmatrix} -A_{i+1}/2 & 0 \\ d\tau\ v_{i+1}/4c_1 & 1/c_1 \end{bmatrix} \qquad (A1.12)$$

$$[H'] = \begin{bmatrix} -\frac{2}{A_{i+1}} & -(\lambda' - \frac{\beta' d\zeta}{2}) & \frac{\lambda' d\zeta}{2} & 0 & 0 & 0 \\ 0 & 0 & 0 & -\frac{d\zeta}{2} & 0_1 & -\frac{1}{2}J_{i+1} \end{bmatrix}$$

(A1.13)

$$\{R\}^T = \langle \bar{V}_{i+1} \quad \bar{v}_{i+1} \quad \bar{a}_{i+1} \quad \bar{V}_{i+2} \quad \bar{v}_{i+2} \quad \bar{a}_{i+2} \rangle, \quad i-1$$

$$\{S\} = \begin{Bmatrix} F(\alpha_j + \alpha_{i-1})d\zeta \\ 0 \end{Bmatrix} \qquad (A1.15)$$

$$[W] = \frac{}{J_{i-2}(\beta' d\zeta^2/2 + \lambda')} \begin{bmatrix} -\lambda' d\zeta/2 & \frac{1}{2}J_{i-2} \\ -(\beta' d\zeta/2 + \lambda') & 0 \end{bmatrix}$$

(A1.16)

$$[N] = \begin{bmatrix} -\frac{d\zeta}{2} & -C_i & -\frac{1}{2}J_{i-2} & 0 & 0 & 0 \\ 0 & 0 & 0 & -\frac{2}{A_{i-1}} & \frac{\lambda' - \beta' d\zeta}{2} & -\frac{\lambda' d\zeta}{2} \end{bmatrix}$$

(A1.17)

$$\{T\}^T = \langle \bar{T}_{i-2} \quad \bar{\tau}_{i-2} \quad \bar{a}_{i-2} \quad \bar{V}_{i-1} \quad \bar{\tau}_{i-1} \quad \bar{a}_{i-1} \rangle$$

(A1.18)

$$\{L'\} = \begin{Bmatrix} 0 \\ -F(\alpha_j + \alpha_{i-1})d\zeta \end{Bmatrix} \qquad (A1.19)$$

APPENDIX - II

BOUNDARY CONDITIONS INVOLVING STEP INPUT

A2.1 PROPAGATION OF DISCONTINUITY

The solution of the system of Equations (2.2 to 2.4 and 2.10) with boundary conditions involving step change in dependent variables ($\bar{a}$, $\bar{v}$, $\bar{V}$, $\bar{M}$) presents complications of the type discussed in Chapter II. For other boundary conditions imposed along each of the two lateral boundaries of the corresponding semi-infinite strip in the half plane $\bar{\tau} > 0$, the solution to the above on an $\bar{x}$-interval of finite length does not present similar problems. The normal derivatives of dependent variables across a physical characteristic may be discontinuous, but these discontinuities do not affect the application of Equations (2.28 and 2.29). However discontinuities in dependent variables are not governed by Equations (2.28 and 2.29). This necessitates the determination, firstly of the line in the half space bounded by finite interval of $\bar{x}$, along which the discontinuities occur, and secondly the magnitude of such discontinuities.

That the discontinuities of dependent variables occur along characteristics may be proved by assuming a

non-characteristic line Γ across which discontinuity exists i.e. between Γ_2 and Γ_1 (Figure A2.1). It is further assumed that in such a region, bounded by Γ_2 and Γ_1, all functions are continuous. Integration of Equation (2.29) with upper sign along $+C_2$ from point 1 to 3 gives

$$\int_1^3 Q^* d\tau + \lambda' (\bar{v}_3 - \bar{v}_1) - \int_1^3 \frac{d\bar{V}}{\bar{A}} = 0 \qquad (A2.1)$$

where

$$Q^* = -\lambda' \bar{a} + \eta' \alpha f + \beta' \bar{v}$$

Assuming Q^* is bounded, as Γ_2 tends to Γ_1 i.e. $d\tau \to 0$, Equation (A2.1) reduces to:

$$\lambda' \delta\bar{v} - \frac{\delta\bar{V}}{\bar{A}} = 0 \qquad (A2.2)$$

Where δ stands for the jump of a particular variable specified.

Similarly, integration along $-C_2$ as $d\tau \to 0$ gives:

$$\lambda' \delta\bar{v} + \frac{\delta\bar{V}}{\bar{A}} = 0 \qquad (A2.3)$$

Combination of Equations (A2.2 and A2.3) yields:

$$\delta\bar{v} = \delta\bar{V} = 0 \qquad (A2.4)$$

Following similar procedure along $\pm C_1$ as $\delta \rightarrow 0$, it can be shown that

$$\delta\bar{M} = \delta\bar{a} = 0 \qquad \text{(A2.5)}$$

The Equations (A2.4 and A2.5) show that the jump across a noncharacteristic line cannot exist.

A2.2 CONDITION OF JUMPS

The condition of jump across a characteristic e.g. $+C_1$ may be obtained by writing Equation (2.28) with lower sign for points 1 and 2 (Figure A2-2). The following Equation showing condition of jump along $+C_1$ is obtained as point 1 tends to point 2

Along $+C_1$:

$$\delta\bar{M} = \frac{\bar{J}}{C_1}\,\delta\bar{a} \qquad \text{(A2.6)}$$

Similarly conditions of jump along the other characteristics may be given as:

Along $-C_1$:

$$\delta\bar{M} = -\frac{\bar{J}}{C_1}\,\delta\bar{a} \qquad \text{(A2.7)}$$

Along $+C_2$:

$$\delta\bar{V} = -\lambda'\,\bar{A}\,\delta\bar{v} \qquad \text{(A2.8)}$$

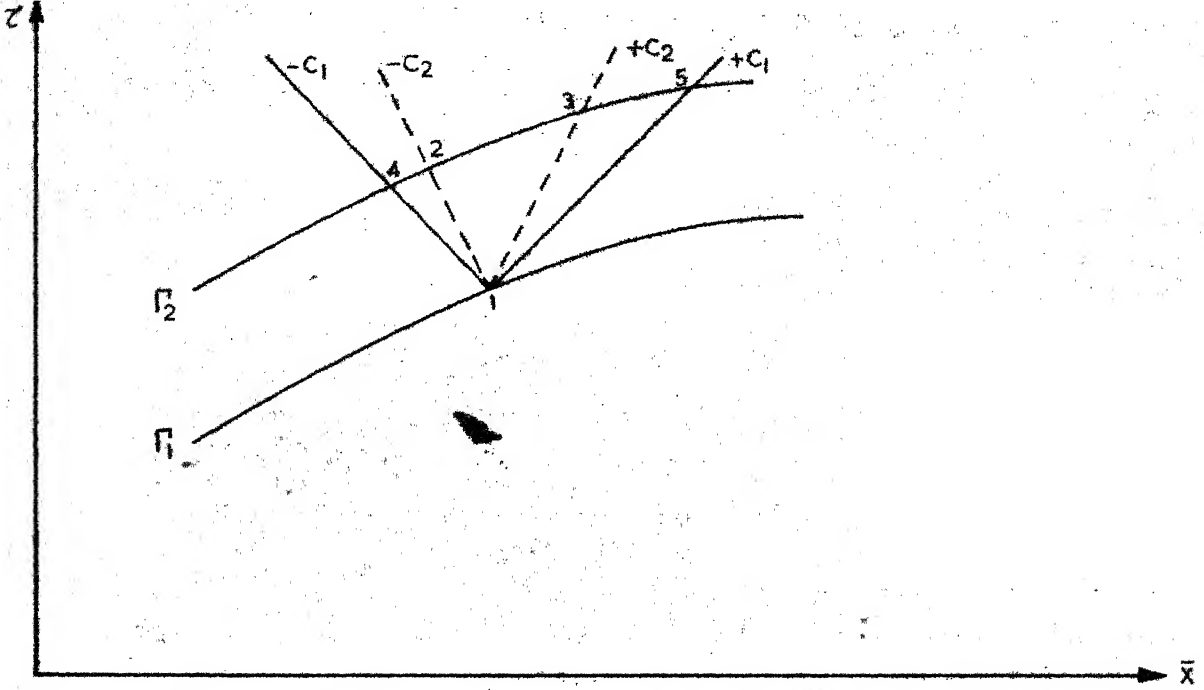

FIG. A 2-1-JUMP ACROSS A NONCHARACTERISTIC LINE

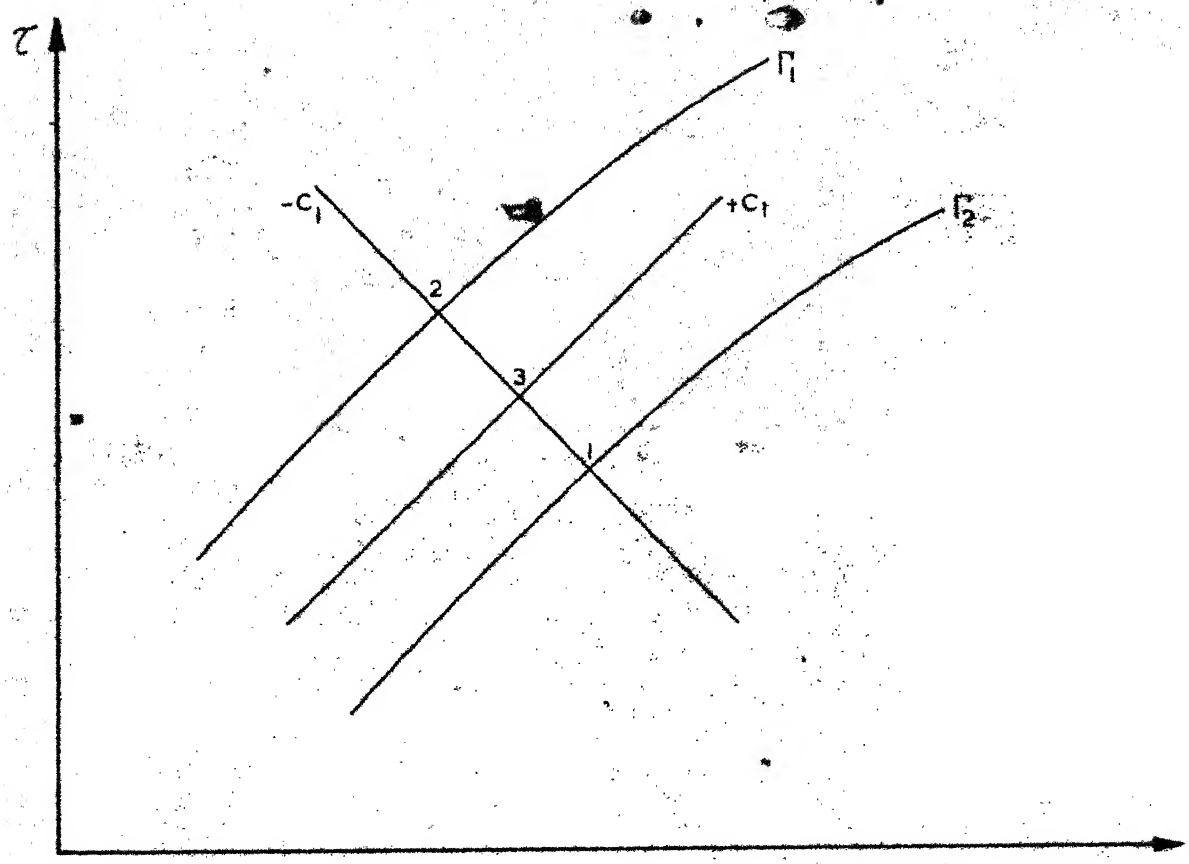

FIG A2-2 JUMP ACROSS A CHARACTERISTIC LINE

Along $-C_2$:

$$\delta\bar{V} = \lambda' \bar{A}\, \delta\bar{v} \qquad (A2.9)$$

The Equations (A2.6 to A2.9) reveal that firstly, discontinuity of $\bar{M}$ is associated with that of $\bar{a}$ and discontinuity of $\bar{V}$ is associated with that of $\bar{v}$, and secondly, discontinuities of $\bar{M}$ and $\bar{V}$ are uncoupled.

A2.3 MAGNITUDE OF JUMP

The magnitude of jump across $+C_1$ may be obtained by writing Equation (2.28) with upper sign for two lines Γ_1 and Γ_2 (with one below and one above $+C_1$) and subtracting one from other. Thus, as Γ_1 tends to Γ_2 gives

$$-\bar{J}\, d(\delta a) - C_1\, d(\delta\bar{M}) = 0$$

Elimination of $\delta\bar{a}$ by Equation (A2.6) yields

$$\frac{\bar{J}}{C_1}\, d(C_1\, \delta\, \bar{M}/\bar{J}) + d(\delta\bar{M}) = 0$$

which after differentiation reduces to

$$\frac{1}{2}\left[\frac{d(\bar{J}/C_1)}{\bar{J}/C_1}\right] = \frac{d(\delta\bar{M})}{\delta\bar{M}} \qquad (A2.10)$$

Solution of Equation (A2.10) may be given by

$$\bar{M}_2 = \bar{M}_1 \left[\frac{(\bar{J}/C_1)_2}{(\bar{J}/C_1)_1} \right]^{1/2} \qquad (A2.11)$$

Where $(\bar{J}/C_1)_2$ indicates value of the same at point 2 which is the upper limit across $+C_1$ and the corresponding lower limit is 1 across $+C_1$.

In a similar way the magnitude of jump across $+C_2$ from point 1 to 2 may be obtained. This is given by

$$V_2 = V_1 \left[\frac{\bar{A}_2}{\bar{A}_1} \right]^{1/2} \qquad (A2.12)$$

It can be very easily verified that the jump across $-C_1$ will be identical with the Equation (A2.11) and jump across $-C_2$ will be identical as the Equation (A2.12).

A2.4 UNIFORM BEAM WITH $k_1 = k_2$

Leonard and Budiansky |1| solved a problem of uniform beam subjected to a jump input $\bar{v}(0, \tau) = 1.0$; $\tau \geq 0$. It was assumed that the material of beam is linearly elastic and possesses a property such that both

waves have the same velocities of propagation (kG = E). The characteristics equation from Equations (2.26 and 2.27) are as the following:

$$\frac{d\bar{\zeta}}{d\bar{x}} = \pm 1 = \pm C_1 \qquad (A2.13)$$

and the condition of jump along the characteristics from Equations (A2.6 to A2.9) are:

Along $+C_1$:

$$\delta\bar{M} = \delta\bar{a} \qquad (A2.14)$$

$$\delta\bar{V} = -\lambda\,\delta\bar{v} \qquad (A2.15)$$

Along $-C_1$:

$$\delta\bar{M} = -\delta\bar{a} \qquad (A2.16)$$

$$\delta\bar{V} = \lambda\,\delta\bar{v} \qquad (A2.17)$$

The magnitude of jump across $\pm C_1$ reduces to

Along $\pm C_1$:

$$\frac{d}{d\bar{\zeta}}(\delta\bar{a}) - 1/2\,(\delta\bar{V}) = 0 \qquad (A2.18)$$

$$\frac{d}{d\bar{\zeta}}(\delta\bar{V}) + \lambda/2(\delta\bar{a}) = 0 \qquad (A2.19)$$

Solution of the system of Equations (A2.18 and A2.19) are

$$\delta\bar{a} = A^* \sin\left(\frac{\sqrt{\lambda}}{2}\tau - C^*\right) \qquad (A2.20)$$

$$\delta\bar{V} = \sqrt{\lambda}\, A^* \cos\left(\frac{\sqrt{\lambda}}{2}\tau - C^*\right) \qquad (A2.21)$$

Where A^* and C^* are constants of integration which are to be determined from the boundary conditions as prescribed in the problem. For the particular problem, for which the boundary conditions are $\bar{v}(0,\tau) = 1$ and $\bar{a}(0,\tau) = 0$ for $\tau > 0$, the constant of integration have the following values

$$A^* = -\sqrt{\lambda}$$

and $$C^* = 0$$

Hence, Equations (A2.20 and A2.21) reduce to

$$\delta\bar{a} = -\sqrt{\lambda} \sin\left(\sqrt{\lambda}\ \bar{x}/2\right) \qquad (A2.22)$$

and $$\delta\bar{V} = -\lambda \cos\left(\sqrt{\lambda}\ \bar{x}/2\right) \qquad (A2.23)$$

Therefore jump of the dependent variables along $+C_1$ is given by

$$\delta\bar{a}(\bar{x},\ \bar{x}) = -\sqrt{\lambda} \sin\left(\sqrt{\lambda}\ \bar{x}/2\right) \qquad (A2.24)$$

$$\delta\bar{V}(\bar{x},\bar{x}) = -\lambda \cos\left(\sqrt{\lambda}\,\bar{x}/2\right) \qquad \text{(A2.25)}$$

The boundary conditions prescribed at the other end are $\bar{M}(1, \tau) = \bar{V}(1, \tau) = 0$ for $\tau \geq 0$. Combination of equations (A2.14 and A2.24) yield

$$\delta\bar{M}(1,1) = \delta\bar{a}(1,1) = -\sqrt{\lambda}\sin\sqrt{\lambda}/2$$

$$\delta V(1,1) = -\lambda\cos\sqrt{\lambda}/2$$

Hence, to satisfy the boundary conditions a jump of variables will occur along $-C_1$ such that

$$\delta\bar{a}(\bar{x},\ 2-\bar{x}) = -\delta\bar{M}(\bar{x},\ 2-\bar{x}) = -\sqrt{\lambda}\sin(\sqrt{\lambda}\,\bar{x}/2) \qquad \text{(A2.26)}$$

$$\delta\bar{V}(\bar{x},\ 2-\bar{x}) = \lambda\,\delta\bar{v}\,(\bar{x},2-\bar{x}) = \lambda\cos(\sqrt{\lambda}\,\bar{x}/2) \qquad \text{(A2.27)}$$

In a similar way it can be shown that

$$\delta\bar{V}(\bar{x},\ 2+\bar{x}) = \lambda\cos(\sqrt{\lambda}\,\bar{x}/2) \qquad \text{(A2.28)}$$

$$\delta\bar{a}(\bar{x},\ 2+\bar{x}) = \sqrt{\lambda}\sin(\sqrt{\lambda}\,\bar{x}/2) \qquad \text{(A2.29)}$$

$$\delta\bar{V}(\bar{x},\ 4-\bar{x}) = -\lambda\cos(\sqrt{\lambda}\,\bar{x}/2) \qquad \text{(A2.30)}$$

$$\delta\bar{a}(\bar{x},\ 4-\bar{x}) = \sqrt{\lambda}\sin(\sqrt{\lambda}\,\bar{x}/2) \qquad \text{(A2.31)}$$

Beyond $\tau = 4$, it can be very easily verified that each interval of $\tau = 4$ will have similar jumps identical to Equations (A2.24 to A2.31).

A2.5 NUMERICAL TECHNIQUE

Numerical technique developed in Chapter III may also be used for the types of problem involving step change of dependent variables. However, additional complications will arise due to tracing of wave fronts (Characteristics) and addition of proper jumps along the wave fronts.

APPENDIX III

BIBLIOGRAPHY AND REFERENCES

1. Leonard, R.W. and Budiansky, B., 'On Travelling Waves in Beams', NACA Technical Report 1173, 1954.

2. Jansman, W.L., 'Propagation of Abrupt Circular Wave Front in Elastic Sheets and Plates', Proceeding of 3rd National Congress of Applied Mechanics 1958, pp. 115-202.

3. Plass, H.J., Jr., 'Some Solution of Timoshenko Beam Equation for Short Pulse Type Loading', Journal of Applied Mechanics, Vol. 25, Trans. ASME, Vol. 80, Sept. 1958, pp. 379-385.

4. Spillers, W.R., 'Wave Progagation of Thin Cylindrical Shell', Journal of Applied Mechanics, Vol. 32, Trans. ASME, Vol. 87, Series E, June 1965, pp. 346-350.

5. Chou, P.C., and Koenig, H.A., 'A Unified Approach to Spherical Elastic Waves by Method of Characteristics', Journal of Applied Mechanics, Vol. 33, Trans. ASME, Vol. 88, Series E, March 1966, pp. 156-168.

6. Chou, P.C. and Mortimer, R.W., 'Solution of One-Dimensional Elastic Wave Problems by the Method of Characteristics', Journal of Applied Mechanics, Vol. 34, Trans. ASME, Vol 89, Series E., September 1967, pp. 745-750.

7. Zanger, C.N., 'Hydrodynamic Pressure on Dams due to Horizontal Earthquake Effects', Engineering Monograph No. 11, U.S. Bureau of Reclamation, May, 1962.

8. Hartree, D.R., 'Some Practical Methods of Using Characteristics in the Calculation of Non-steady Compressible Flow', Report LA-HU-1, Department of Mathematics, Harvard Univ., Cambridge.

9. Courant, R., Hilbert, D., 'Method of Mathematical Physics, Vol. 2, Interscience Publisher Inc., New York.

10. Courant, R., Friedrichs, K. and Lewy, H., 'Uber die Partiellen Differenzengleichnngen der mathematishem Physink', Math. Ann. Vol. 100, pp. 32-74.

11. Sauer, R., 'Anfangswer probleme bei Partiellen Differential gleichungen', Springer Verlag, Berling 229, pp. 44, 49, 64-67.

12. Timeshenko, S., 'Vibration Problem in Engineering, Van Norstrand.

13. Forsythe, G.E., and Wasow, W.R., Finite Difference Methods for Partial Differential Equation, John Wiley and Sons, Inc., New York.

14. Hilderbrand, F.B., Finite Difference Equations and Simulations, Prentice Hall, Inc. Englewood Cliffs, New Versy.